

CHAPTER 1

INTRODUCTION

1.1 Background of Study

The research project involves design and analysis of an in-wheel motor system for retrofit installation into non-hybrid vehicles. When the in-wheel motor systems and the other subsystem such as the energy storage, motor controllers, and energy management systems are all installed inside the vehicle, the vehicle can operate as a hybrid electric vehicle. In addition, the proposed in-wheel motor system can also be used for other types of vehicle platforms such as series hybrid electric vehicle, electric vehicle and fuel cell vehicle.

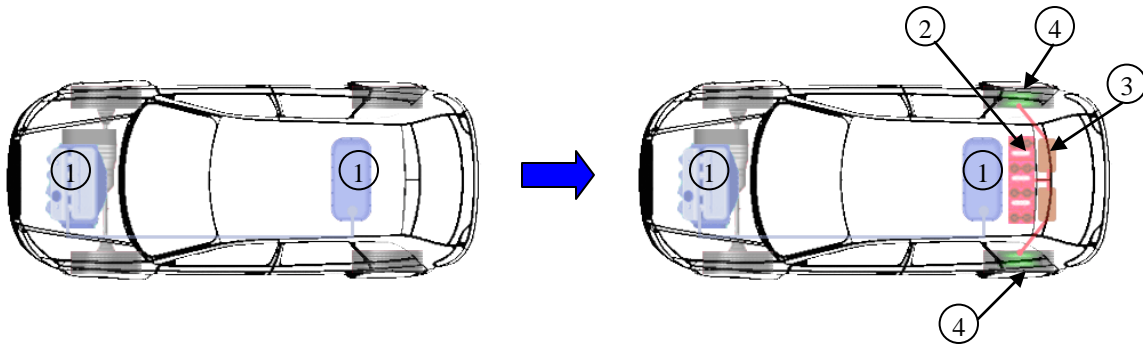


Figure 1.1: Retrofitting Process of a non-HEV with In-Wheel Motors and other systems
(1 – original system (fuel tank & engine), 2 – batteries, 3 – motor controller, 4 – in-wheel motors)

Globally, transportation systems have significant impacts on the environment, accounting for between 20% and 25% of world energy consumption and carbon dioxide emissions [1]. Therefore, to reduce the adverse impact of transportation systems towards the environment, the efficiency of the vehicle propulsion systems has to be increased. Hybrid vehicles are identified as one of the potential solution towards sustainable transportation systems by Partnership for New Generation of Vehicles, USA [2]. Among the alternative vehicle propulsion options considered to reduce dependency on the petroleum are hybrid electric vehicle (HEV), fuel cell vehicle (FCV), solar vehicle and full electric vehicle (EV). In all of these three options or vehicle platforms, the in-wheel motor systems can be installed to

provide traction to the wheels instead of installing an on-board chassis mounted electric motors. Several examples of the in-wheel motor application had been demonstrated in prototype stage [3] and the future seems bright for in-wheel motor applications.

This project is focusing on the development of an In-Wheel Motor (IWM), which is based on axial flux permanent magnet motor topology. There are several types of in-wheel motors being developed for passenger cars and larger vehicles, almost all of these motors are still at prototype stages. The only types of in-wheel motors available in the market at present are for smaller scale applications such as for solar cars [4] and motorized wheel chairs [5] or for larger scale applications on electric buses (still at trial stage [6]). Therefore the opportunity to develop an in-wheel motor system for the target vehicle applications (passenger car size) still exists at the moment considering all the demonstrated versions are still in various prototype stages.

1.2 Problem Statement

In-wheel motor can be installed within the wheels of non-hybrid vehicles as a retrofit system. The main challenges in designing such retrofit system are the space limitation and interfacing with the present components and suspension hard points since the vehicle is not originally designed for it.

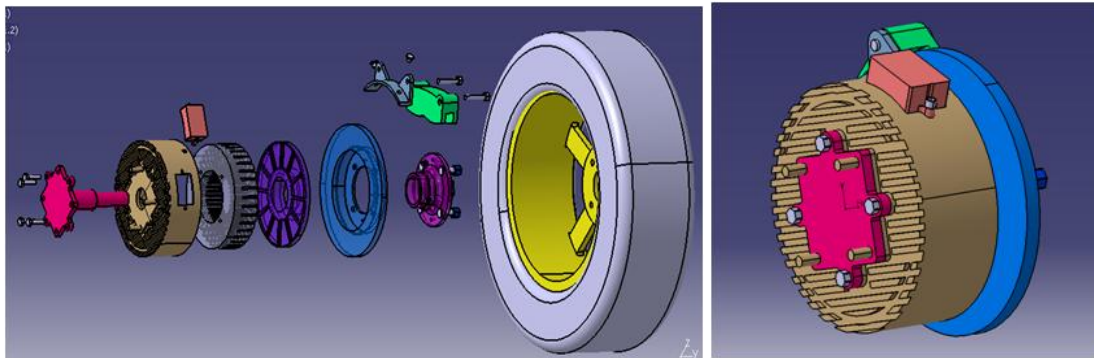


Figure 1.2: UTP In-Wheel Motor Design 1 – previous design

There are several problems exists with the existing design of the in-wheel moor shown in Figure 1.2. The main problem is the small design envelope of only 150 mm in diameter (limited by the interference with stock braking system) by 100 mm in thickness (maximum width where the whole assembly still remain inside the wheel arch of the car), which

theoretically allows for only 4 kW of power output with current manufacturing capability, materials availabilities, limit on the maximum field strength of the rare earth permanent magnet and the heat sink design. The new design of the in-wheel motor will address some of these problems by looking at a new type of brake system design which allows larger design envelope (up to 300 mm radially), hence allowing larger power output to be achieved (15 kW peak power per motor).

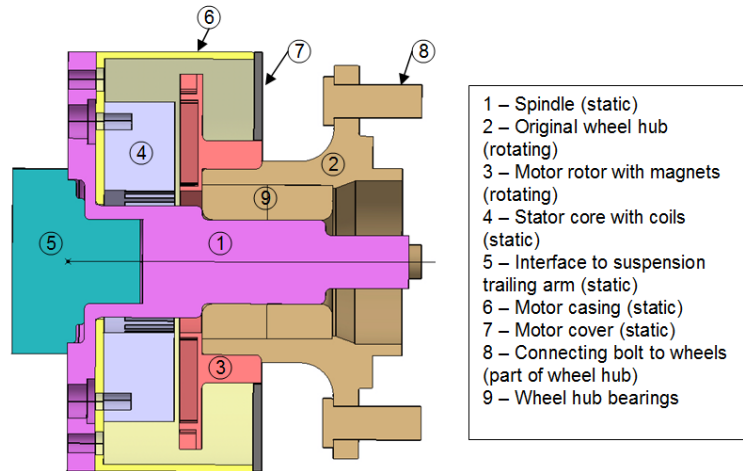


Figure 1.3: Cross section view of the current in-wheel motor design (Design 1)

There are two possible solutions available to address this problem, which are by using compact axial flux motor and new disc rotor braking system.

1.3 Objectives

There are two main objectives of this project, which are i. to design and analyze a compact in wheel motor for retrofitting installation into a non-hybrid cars, and ii. to design and analyze a new disc rotor braking system for the said in-wheel motor systems.

Fitting an in-wheel motor to each wheel produces an all-wheel drive system that eliminates the needs for transmission, drive shafts, differential gears or other complex mechanical components. In addition, the in-wheel motor makes it possible to control drive torque and braking force independently and with great precision at each wheel [7]. However, the in-wheel motor also introduces additional challenges in terms of additional unsprung

mass effect on vehicle performance, limited design envelope available for packaging around the existing systems, ability of the new braking system (new disc rotor and regenerative) to provide sufficient braking performance, heat dissipation from the motor and heat transfer performance of the whole system, manufacturing options of the components and cost reduction.

1.4 Scope of Study

This project involves research, design, analysis, fabrication study (actual fabrication to be outsourced to an outside manufacturer) and testing of a prototype in-wheel motor with new disc braking system designed for retrofitting purpose on a non-hybrid electric vehicle. In order to reduce total thickness of the system, a new disc rotor braking system is suggested as a replacement for the stock disc brake or drum brake system. The scope of the project only involves mechanical engineering works and expected to work with other researchers who are involved in the electromagnetic design of the electric motor and the motor drive system.

The final output of the project will be final design specification and a 3-dimensional model of the proposed system..

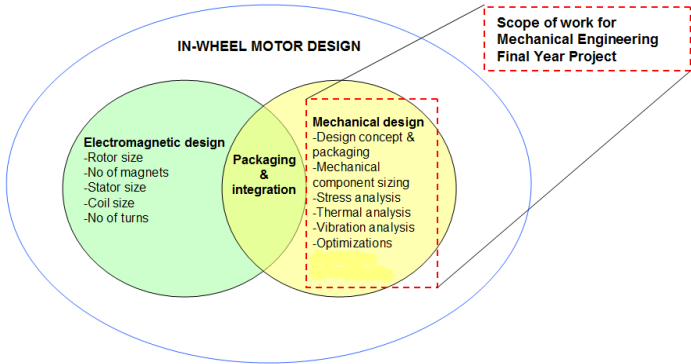


Figure 1.4: Scope of Work for FYP as part of overall motor design project

CHAPTER 2

LITERATURE REVIEW AND THEORY

Most of tasks project utilize basic principals in engineering, especially in component design. The information such as the basic typical of hybrid electric vehicle, application and efficiency of axial flux permanent magnet, and basic design of rotor are very important to know and review as a source to re-design a new In-Wheel Motor.

2.1 In-Wheel Motor

The basic principle behind a vehicle equipped with in-wheel electric motors is simple. The most basic design is a rather simple integration of an electric motor into the hub of the wheel. When power is applied to the stationary coils on the inside of the wheel, an electromagnetic field is generated and the outer part of the motor attempts to follow it and turns the wheel to which it is attached [8].

Example of In-Wheel Motors:

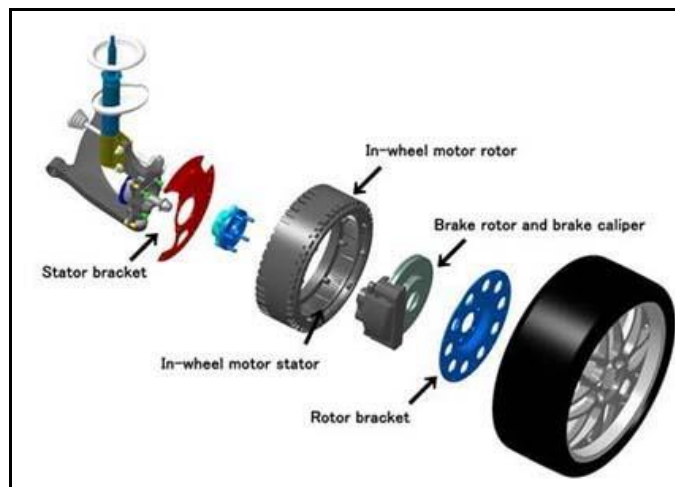


Figure 2.1: Mitsubishi MIEV In-Wheel Motor [7]

The use of an outer rotor boosts maximum torque and eliminates the need for a reducer unit. The reduction in overall size also allows the motor to be fitted in the front wheels.

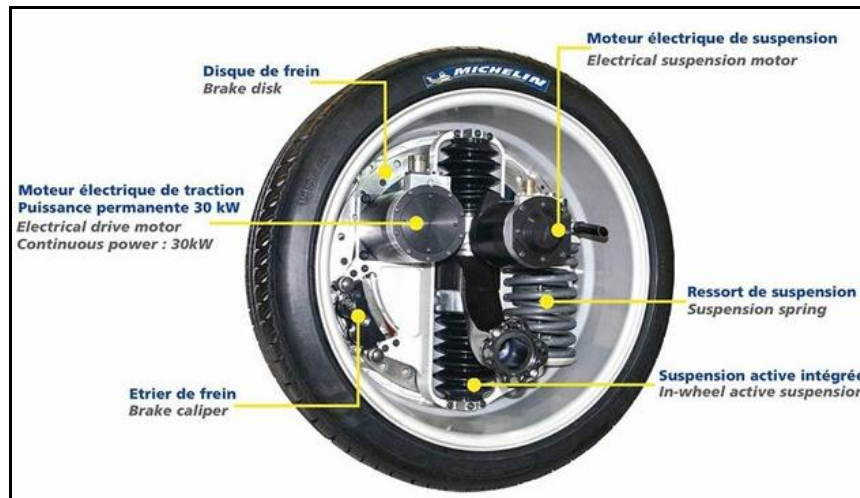


Figure 2.2: Michelin In-Wheel Motor Concept [8]

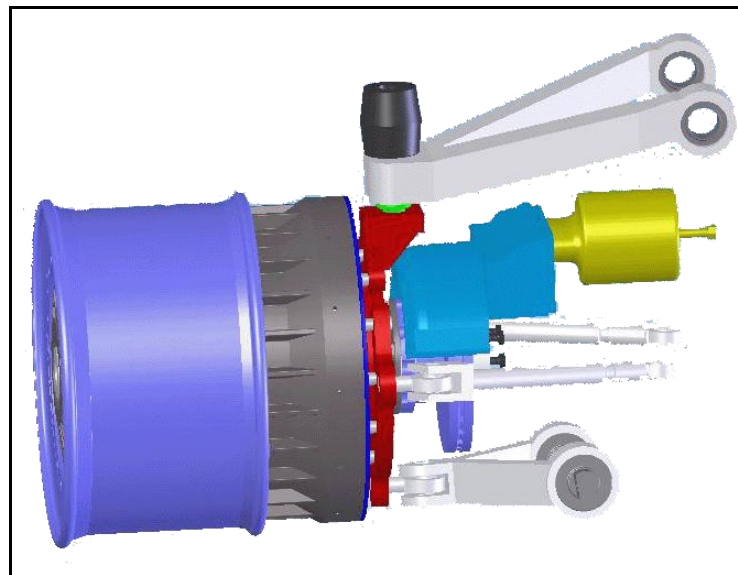


Figure 2.3: E-Traction in-wheel motor for electric bus

On a vehicle equipped with in-wheel electric motors, several major systems are housed within the wheel itself. So, it only stands to reason that many of the core components of a traditional automobile can be removed. The engine, transmission, clutch, suspension and

other related parts can be eliminated on vehicles equipped with in-wheel electric motors because the in-wheel components handle all of these functions.

2.2 Brake Systems – Mechanical and Regenerative Braking

2.2.1 Mechanical Braking System

The braking system is a means of converting the vehicles momentum (called kinetic energy) into heat by creating friction in the wheel brakes. The heat then dissipated into the air, and it is ability to absorb and dissipate heat that prevents brake fade under severe conditions. In conventional mechanical brakes in which the braking torque is received directly by a stationary member, the braking effect is usually insufficient because no self-energizing force is generated, and they need many mechanical elements which cause considerable friction.

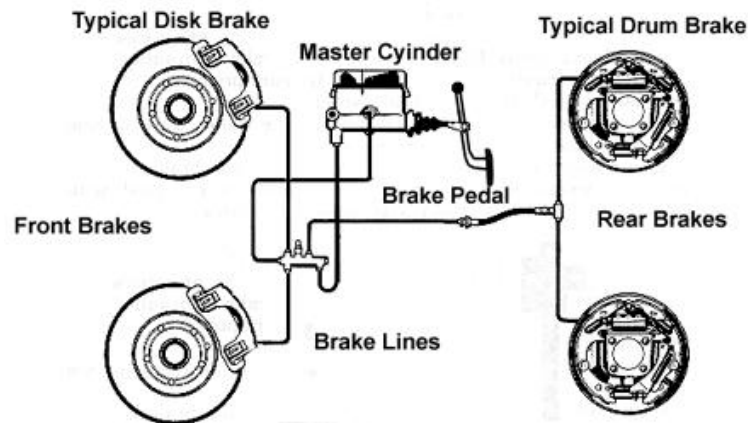


Figure 2.4: Typical Mechanical Braking System

The typical brake system consists of disk brakes in front and either disk or drum brakes in the rear connected by a system of tubes and hoses that link the brake at each wheel to the master cylinder. Other systems that are connected with the brake system include the parking brakes, power brake booster and the anti-lock system.

Basic Equations in Mechanical Braking System [9]:

Torque created by the caliper on the rotor (at the wheel) = T_w

$$T_w = P_s \times A_p \times \mu \times 2 \times R_E$$

Where;

P_s – Pressure of system

A_p – Total area of pistons in one half of caliper (one side of opposed type or active (piston) side of sliding or floater type)

R_E – Effective radius of clamping force

μ - Friction coefficient; x 2 since there are two sides of the rotor that the pads are exerting against

2.2.2 Electrical Regenerative Brake System

A regenerative brake is an energy recovery mechanism that reduces vehicle speed by converting some of its kinetic energy into a storable form of energy instead of dissipating it as heat as with a conventional brake [10]. The captured energy is stored for future use or fed back into a power system for use by other vehicles. With regenerative brake, the system that drives the vehicle does the majority of the braking. Example is on electric or hybrid vehicle when the driver step on the brake pedal, these types of brakes put the vehicle's electric motor into regenerative mode, causing it to introduce load on the car as the motor is now acting as a generator, thus slowing the car's wheels. The electricity produced is then fed into the vehicle's batteries.

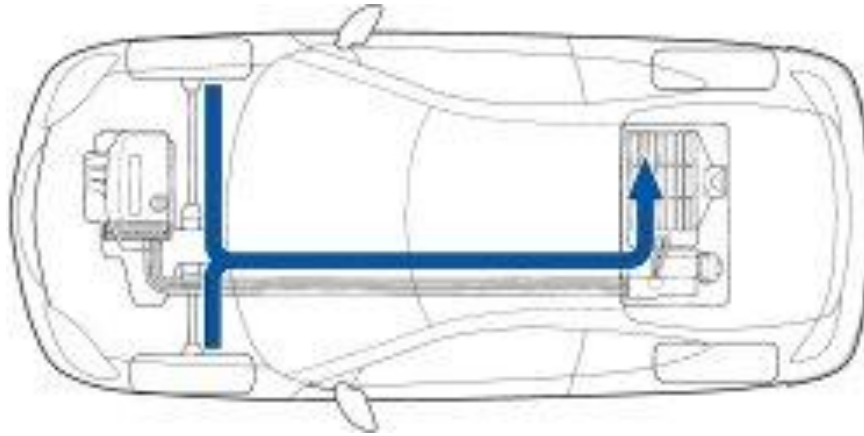


Figure 2.5: Regenerative Braking in Honda Insight – Energy captured stored in the batteries

[11]

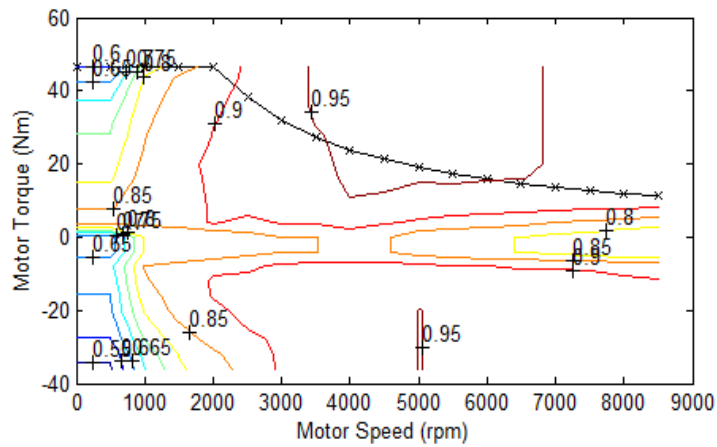


Figure 2.6: Honda Insight Torque curve – negative torque used for regenerative braking

In Figure 2.6, the negative torque shown on the graph is actually the available braking torque produced by the electric motor in regenerative braking mode. Typically the magnitude of braking torque in regenerative mode is less compared to the driving mode due to the limit on the maximum amount of current batteries can absorb in charging mode [10].

2.3 In-Wheel Motors in Different Vehicle Platforms

Mitsubishi Motors is one of the automotive manufacturer that try to apply In-Wheel Motor for three different vehicle platforms which are Series Hybrid Electric Vehicle (SHEV), Electric Vehicle and Fuel Cell Vehicle (FCV) as shown in the figure below.

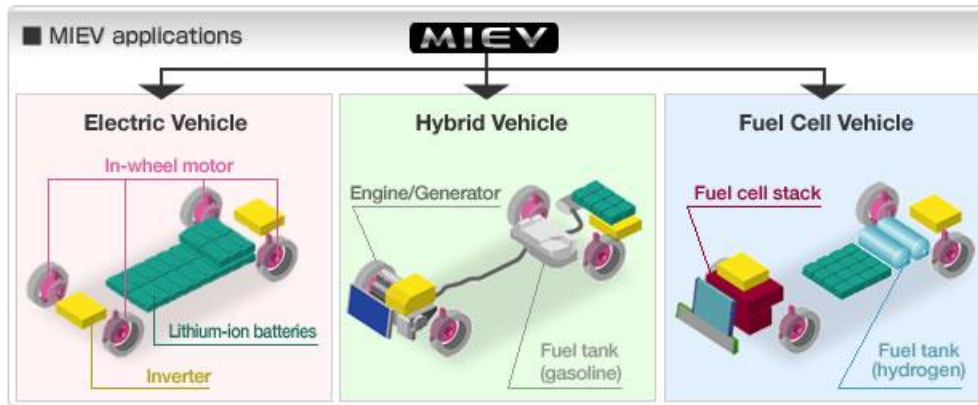


Figure 2.7: MIEV applications [7]

2.3.1 Series Hybrid Electric Vehicles

The series hybrid electric vehicle has its wheels driven only by an electric motor powered by a battery, with an engine plant that provides electric power to the battery and if necessary to the electric drive.

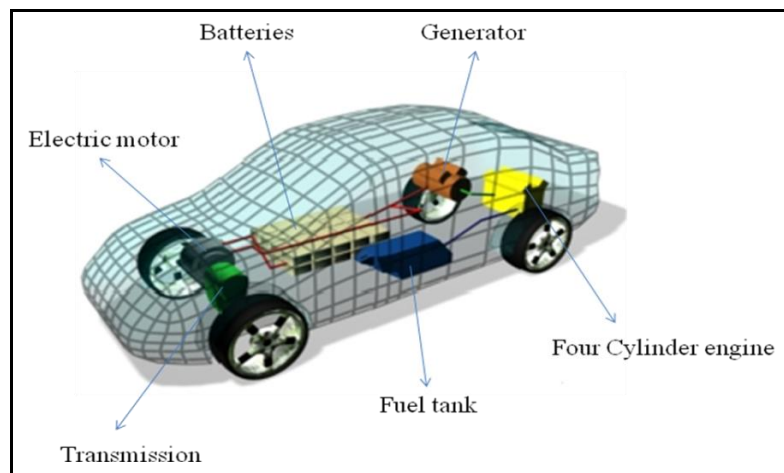


Figure 2.8: Typical Series Hybrid

Description of each component:

- Electric motor – Provide the propulsion power
- Transmission – Similar to transmission in electric vehicle, the motor can spin fast enough so that the transmission only need one gear
- Batteries – Store Energy recovered from braking or generated by the motor
- Fuel tank – The main energy-storage device for hybrid
- Generator – Gas engine power gets converted to electrical power to drive the motor
- Four cylinder engine – The engine on a series hybrid turns the generator

2.3.2 Electric Vehicles

An electric vehicle (EV), also referred to as an electric drive vehicle, is a vehicle which uses one or more electric motors for propulsion. As according to the above information about Mitsubishi technology, there are also developing in wheel motor for Electric Vehicle usage.



Figure 2.9: In-Wheel Motor (on Mitsubishi Colt EV) [7]

2.3.3 Fuel Cell Vehicles

A Fuel cell vehicle or FC vehicle (FCV) is any vehicle that uses a fuel cell to produce its on-board motive power. Fuel cells on board the FC hydrogen vehicles create

electricity to power an electric motor using hydrogen fuel and oxygen from the air. A fuel cell process produces only water and heat.

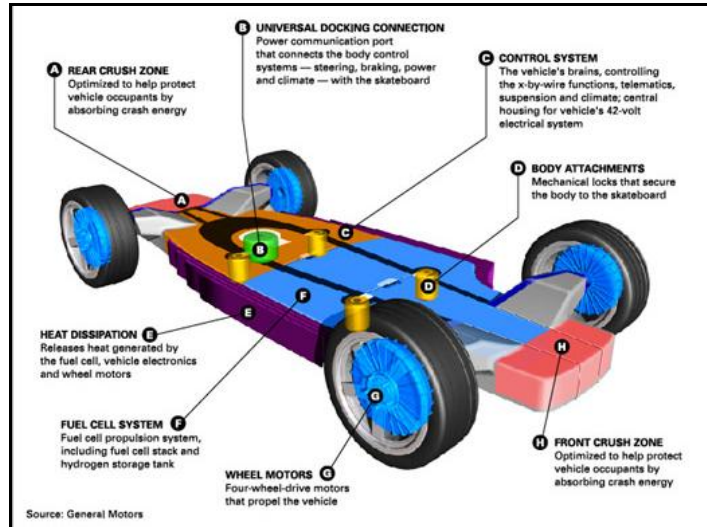


Figure 2.10: General Motors Fuel Cell Autonomy Concept with In-Wheel Motors [12]

2.4 Axial Flux Permanent Magnet

The Axial flux (Permanent Magnetic) motor is an attractive alternative to the cylindrical radial flux motor due to its compact construction and high density. They have become widely used for speed control applications. Axial flux PM motor also called disk-type motors can be designed as double-sided or single-sided machine, with internal or external PM rotors and surface mounted or interior type PMs.

As the output power of the axial flux motor increases, the contact surface between rotor and shaft become smaller. Careful attention must be given to the design of the rotor-shaft mechanical joint as this is the principal cause of failure of disk type motors.

The Axial Flux (PM) motor has the highest power density compared to other design topologies of electric motor [13]. In axial flux motor the electromagnetic flux path is in axial direction parallel to the shaft axis. The torque is generated from the inside of the inner radius to the edge of outer radius of the motor rotor., compared with radial flux motor where torque generation occur only at the radius of the air gap. Therefore, in most applications the axial

flux motor typically exhibit the highest peak power and peak torque per volume ratio compared with the radial flux motor.

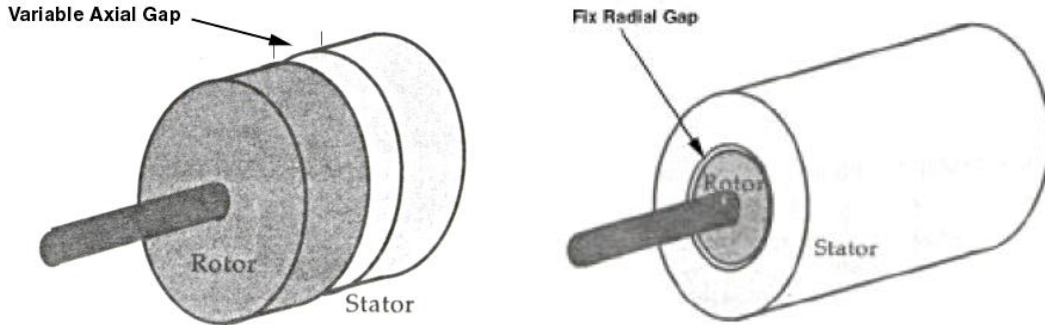


Figure 2.11: Comparison of axial flux motor (left) and radial flux motor (right)

In general, the peak torque of the motor is a function of several important motor design parameters which are; average strength of the magnetic field in the air gap - B_{avg} , current density - A , active surface of permanent magnets - $\pi(R_o^2 - R_i^2)$ and several other design factors. However, the equation below [14] can give a good estimation of peak torque available from a single stator axial flux motor given the fix dimensions or design envelope.

$$\text{Torque, } T = F.R_i = B_{avg}A\pi(R_o^2 - R_i^2)R_i$$

Where;

F – Electromagnetic force developed

R_i – inner radius of the motor

B_{avg} – average magnetic field strength in the air gap

R_o – Outer radius of the motor

A – Current line density

CHAPTER 3

METHODOLOGY

3.1 Methodology

This main task of this project can be separated into three main processes, which are design, analysis and design iterations for optimization. In the design stage, literature review is important at the preliminary stage resulting from summarize current methods and models to identify the best design for analysis and design iteration in the future.

In order to ensure that the information is within the research topic, objectives and problem statement must be fully understood. Relevant literature review is required on the topics of axial flux motor design, hybrid electric vehicles, braking systems and mechanical design equations to help assist with the decisions on components' dimensions, sizes and material. Software training will run in parallel until the analysis stage starts. Then 3D modeling using CATIA or any software with the same function will start right after the specification of the motor obtained from the design equation.

The second process is the analysis stage; this stage requires three types of analysis, which are the analytical analysis, finite element stress analysis and finite element thermal analysis. Analytical analysis to determine the component sizing was completed in the first stage of the project (FYP 1) and the finite element analyses were performed in the second stage of the project (FYP 2).

Then comes to final stage which is the design iterations consist of three major part; preliminary, critical and final design reviews. After that, run finite element stress and thermal for the best design. The next section shows all the main activities of the project in the activity network format. With the use of activity network, the critical points or activities can be identified early. The critical points are when there exists a convergence of activities towards those points and the completion of the task involved in the critical points is necessary in order to proceed to the next stage. For FYP I, three critical points are identified (and

completed) which are; i. Determination of Target Design Specifications, ii. Design Selection from Concepts and iii. Design Process.

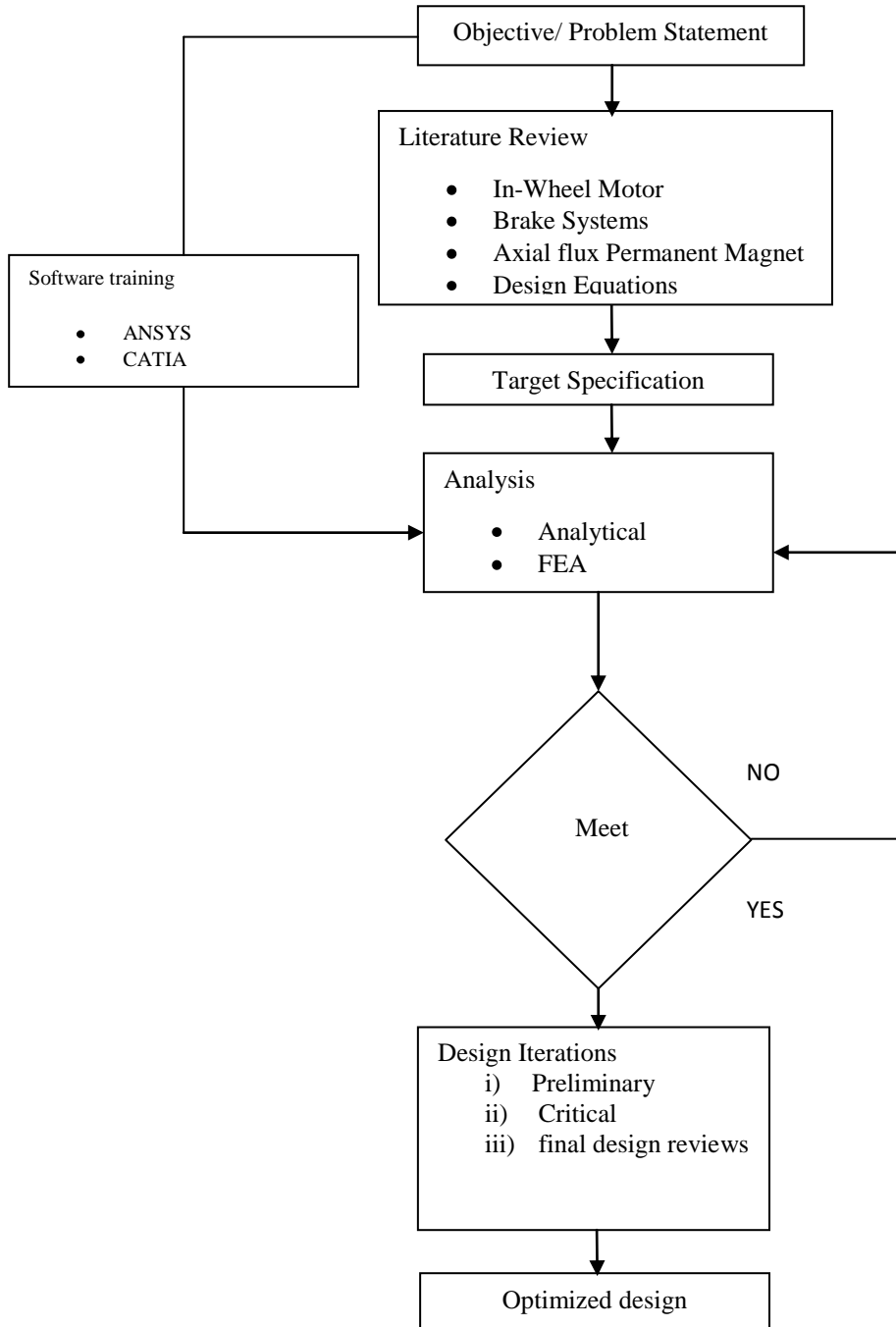


Figure 3.1: Flow Chart

3.2 The Project Flow – Activity Network

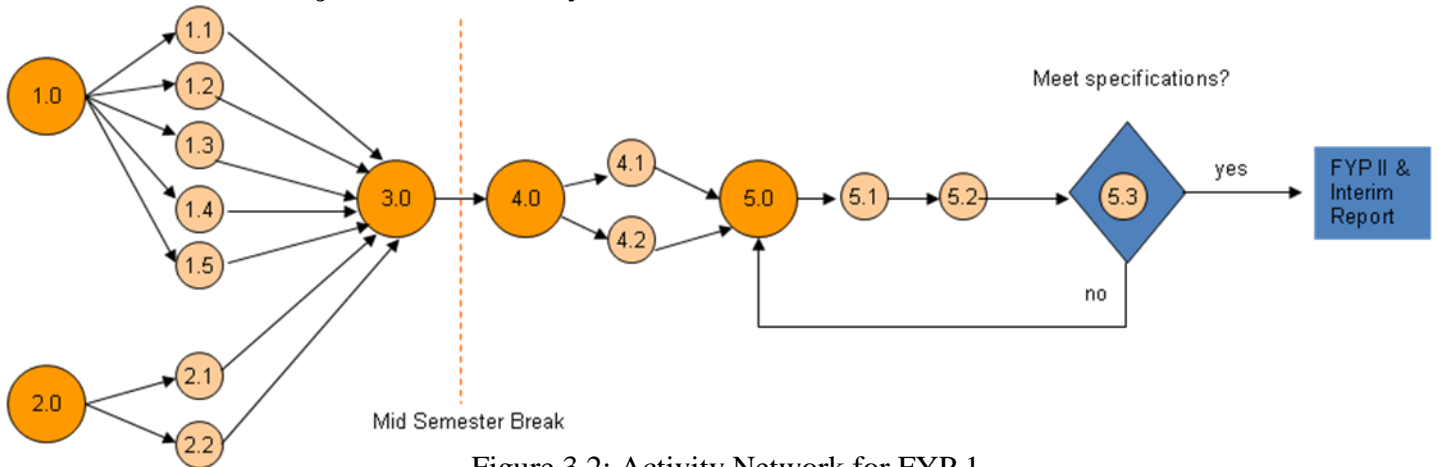


Figure 3.2: Activity Network for FYP 1

Task List for Activity Network of FYP 1

1.0 Literature Review

- 1.1 Hybrid Electric/Fuel Cell/Electric Vehicles
- 1.2 In-Wheel Motor
- 1.3 Vehicle Dynamics
- 1.4 Brake System Design & New disc Braking System
- 1.5 Axial Flux Permanent Magnet Motor

2.0 Data Gathering (not completed - CM machine breakdown, manual measurements done)

- 2.1 Suspension components & design envelope digitization
- 2.2 Vehicle body, weight distribution & CGH (center of gravity height)

3.0 Target Design Specifications (CRITICAL POINT)

4.0 Design Selection (CRITICAL POINT)

- 4.1 Comparison of Design Concepts
- 4.2 Decision Matrix

5.0 Design Process (CRITICAL POINT)

- 5.1 Component Sizing – analytical calculation
- 5.2 Component analysis & refinement – FEA tools
- 5.3 3D model analysis

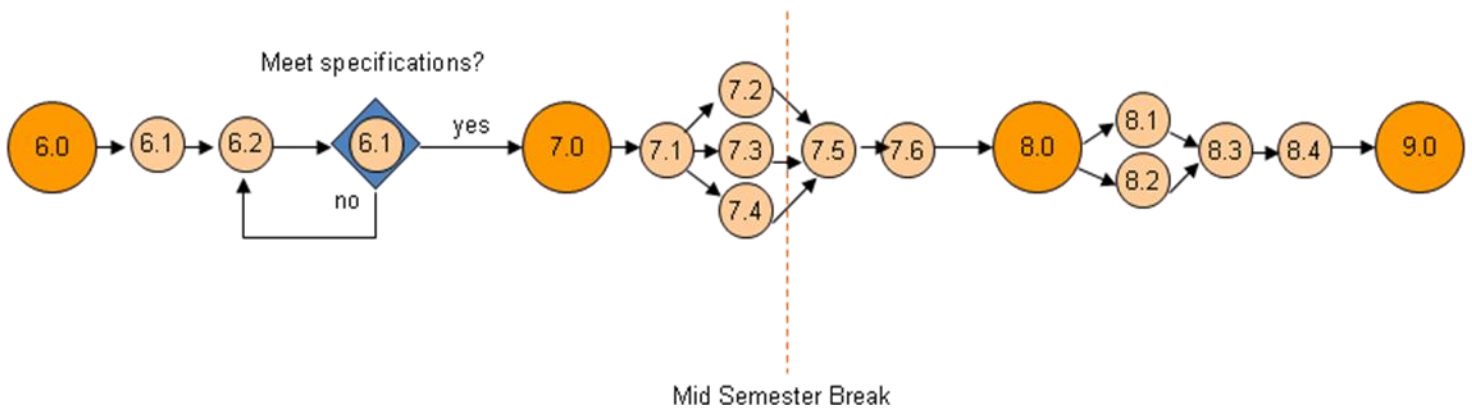


Figure 3.3: Activity Network for FYP 2

Task List for Activity Network of FYP II

6.0 Design Optimization

6.1 List of parameters for design optimization

6.2 Specifications for design optimizations – performance, cost, strength, weight, etc

6.3 Design optimizations using FEA tools

7.0 Design Iterations

7.1 3D Models & Assembly Analysis

7.2 Preliminary

7.3 Critical

7.4 Final design Review

7.5 Technical Drawing

7.6 Modification

8.0 Type of analysis

8.1 Finite Element Stress

8.2 Finite Element thermal

8.3 Finalize the analysis

8.4 Data Analysis & Discussion

9.0 Technical Report

9.1 Report of Task 1-8

9.2 Recommendations

3.3 In-Wheel Motor Target Specifications

Table 3.1 shows the target specifications of the in-wheel motor and Figure shows the estimated maximum torque from the motor. In designing some of the components such as the rotor of the motor, the maximum load acting on these components is actually from internal, which is the motor torque itself. Based on the motor power output of 15 kW, it is also estimated that the maximum heat loss will be around 20% which is 3 kW of heat dissipation from the motor.

Table 3.1: Summary of Motor Specifications

No	Item	Parameters/Targets
1	Motor size – design envelope of rotor & stator	OD = 240 mm, Thickness = 80 mm
2	Maximum torque, top speed, peak power (per motor)	120 N.m, 1381 rpm, 15 kW
3	Motor topology	Axial Flux PM motor, single stator, salient pole coils, 3-phase Y-configuration
4	Motor Controller	108 VDC, 240 amps, sinusoidal 3 phase controller, MOSFETs
5	Estimated motor mass	Less than 25 kg
6	Maximum top speed in electric vehicle (EV) mode – traction from motors only	100 km/h
7	Maximum speed for assist mode (HEV)	140 km/h

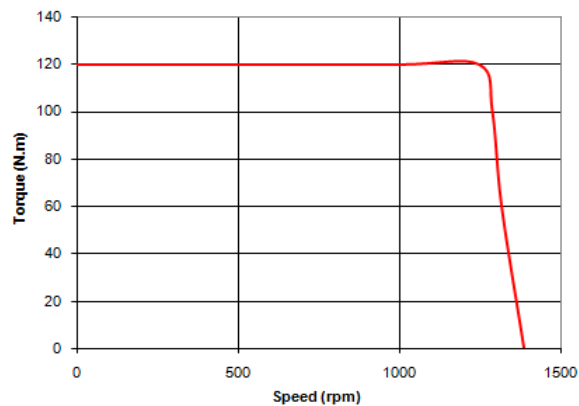


Figure 3.4: Estimated Maximum Torque Speed Performance of a 15 kW In-Wheel Motor

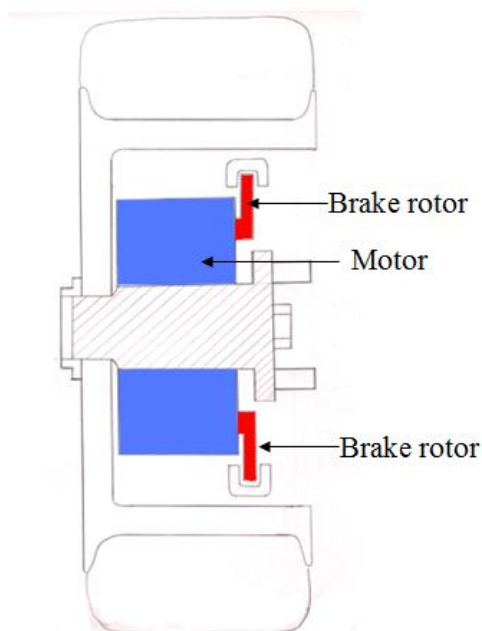
CHAPTER 4

RESULTS AND DISCUSSION

In order to arrive at the final design of In-Wheel Motor several steps are required the first step is gathering of vehicle data such as: vehicle mass and weight distribution gathered. The second step is design selection based on several possible concepts. The selection is done by using a decision matrix, which compares the different concepts according to several selection criterias. The third step involves critical component sizing using analytical stress equations based on expected loadings during normal and extreme operations (most likely to be encountered). The fourth step is the 3-dimensional modeling of the selected design based on the preliminary calculations of the critical components sizing. The fifth step is the finite element analysis on each component in order to optimize the design of the components. In parallel to all the activities of steps above, brake design calculations were also performed to determine the proper sizing of the new mechanical brake components as well as the component sizing.

4.1 Design Iterations

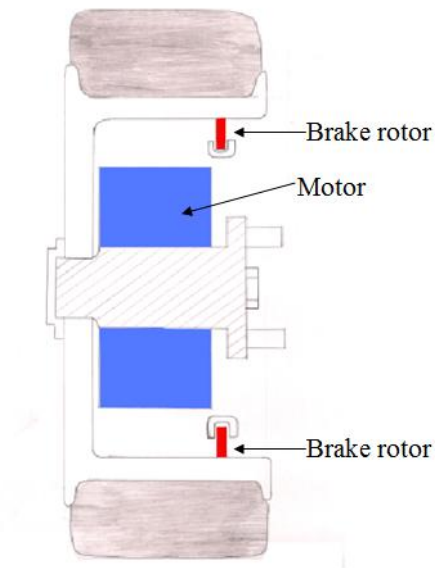
First Concept



Description:

This is the first basic design which the motor outside but the rotor is on the motor

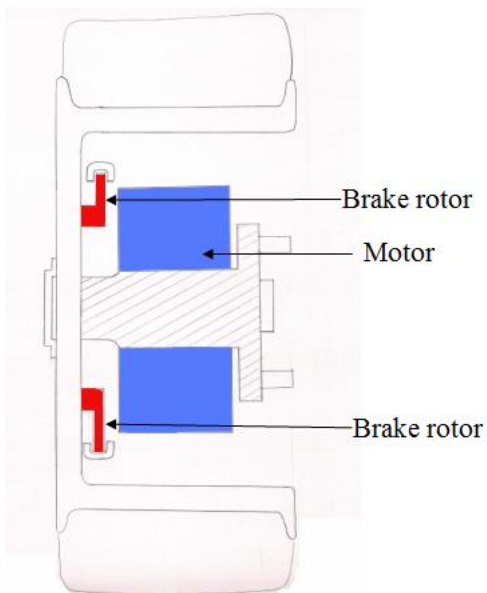
Second Concept



Description:

Some modification are made which the brake disc is on the rim but the motor at outside

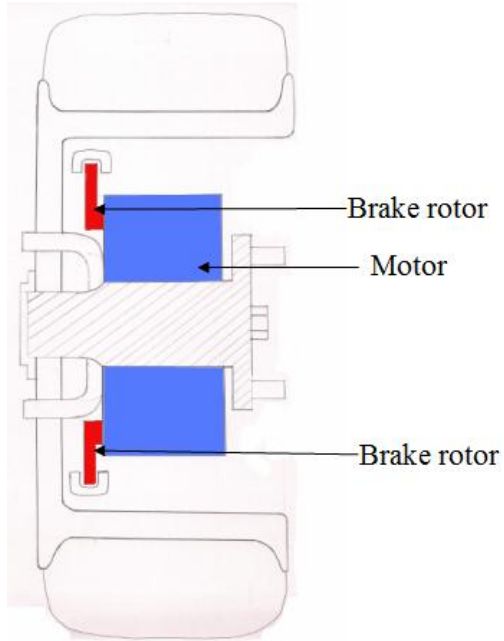
Third Concept



Description:

Motor inside meanwhile the brake disc is on the rim

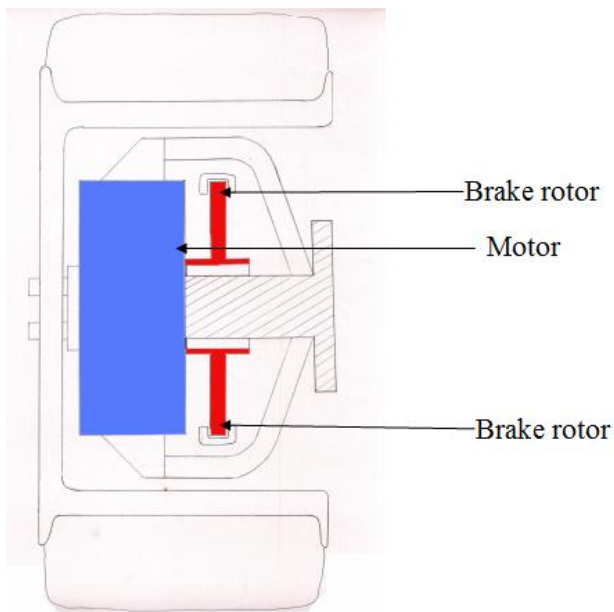
Fourth Concept



Description:

Brake disc is on the motor inside

Fifth Concept



Description:

Different from above concept which is have arms that mounted on the outside motor

4.2 Decision Matrix – Design Selection Process

In order to make the decision of the best design concept, five important factors need to be considered:

1) Performance

- Motor torque output
- Braking performance
- Vehicle Dynamic

2) Reduce complexity

- Less no of parts
- Easier to manufacturing
- Easier to assembly
- Easier maintenance

3) Total mass

- Total of each component

4) Cost

- Material used
- Fabrication process
- Assembly
- Maintenance

5) Retrofitability

- Can be integrated easily to non-hybrid vehicle
- Less modifications to existing vehicle

For each factor are given different percentage based on the level of advantages or disadvantages to be multiply with the weightage. The highest total of the result will be decided as the best design concept and it goes to fifth design concept.

Table 4.1: Design Specification for each component

Concepts			Concept	(x)								
Specifications		Weightage	1	Weightage	2	weightage	3	weightage	4	weightage	5	weightage
Performance (%)	Torque	3	100	300	100	300	100	300	100	300	100	300
	Braking		100	300	100	300	100	300	100	300	100	300
	Dynamic		75	225	75	225	70	210	70	210	80	240
Reduce Complexity easier~5 easy~3 difficult~1	No of Part, Manufacturin g, assembly, Maintainance	5	easy	15	easy	15	easier	25	easier	25	easy	15
Total Mass heavy~5 medium~3 less~1	Submission of the components	4	medium	12								
Cost High~5 Medium~3 Low~1	Material, Fabrication process, Assembly, Maintainance	5	medium	15								
Retrofitability Suitable~5 moderate~3 Not Suitable~1	i) Integrated to non-hybrid vehicle ii) Less modifications to the existing vehicle	4	moderate	12	moderate	12	moderate	12	moderate	12	Suitable	15
Total				279		279		274		274		297

CATIA 3D Drawings (Design A):

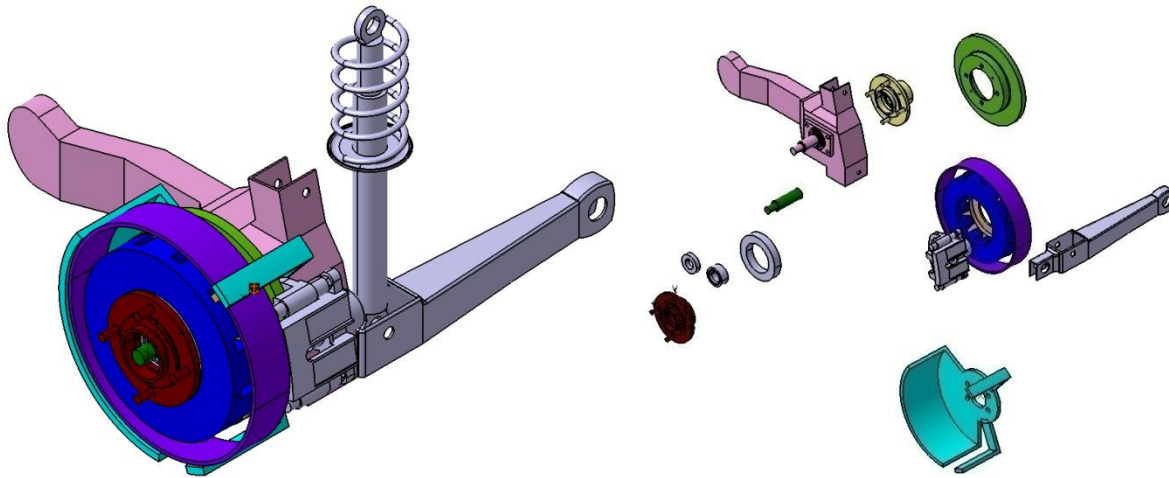


Figure 4.1: Isometric View and Exploded View of the In-Wheel Motor Assembly

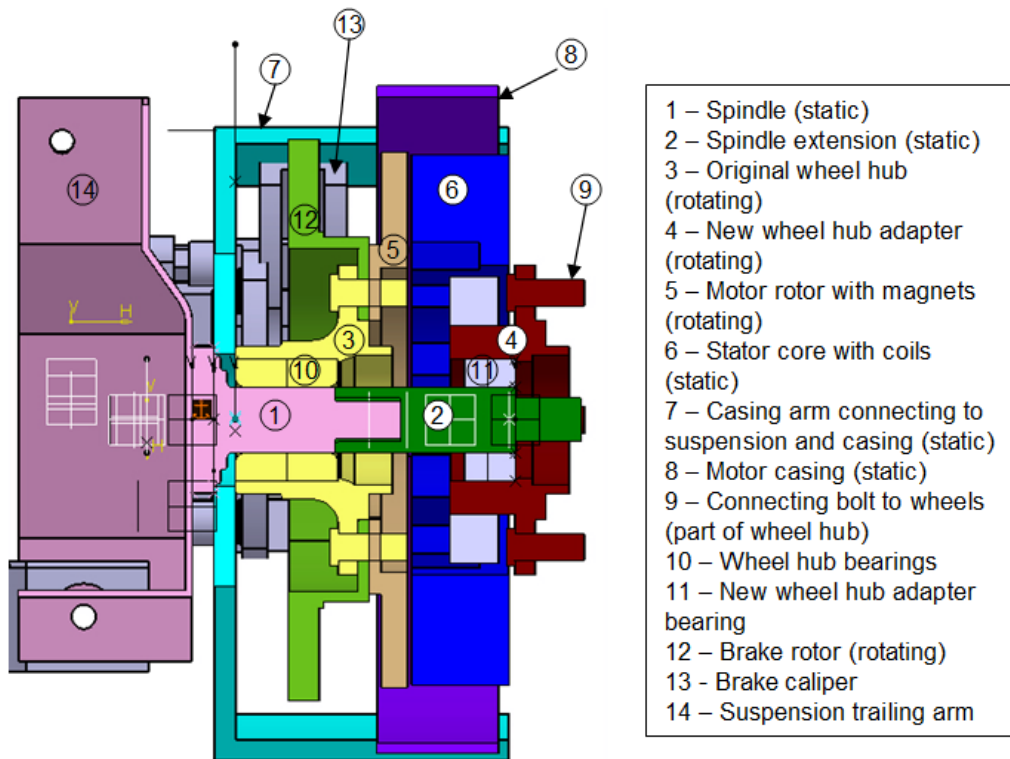


Figure 4.2: Section view of the In-Wheel motor assembly

4.3 Analytical Stress Analysis

4.3.1 Boundary Conditions/Loadings

The first step is to determine the sizing of the components based on the expected loadings during normal (example: static weight, cornering, braking, etc) and extreme operations (example: minor impact). Based on these loading conditions, the size requirements and also materials required can be estimated before optimizing the design further using finite element analysis method. There are several boundary or loading conditions, which need to be considered in order to calculate stress on the components which are:

- i) Static load (under vehicle own weight)

Assumption: For ease of calculation & component sizing, assume uniform weight distribution

$$F = (M_v/4) \times g \quad ; M_v = 1300\text{kg} \quad g = 9.81 \text{ m/s}^2$$

$$F = 3188.25 \text{ N}$$

- ii) Vertical Impact (Hitting a pothole)

Assumption: 2g vertical impact

Vertical force = Static Force x 2g

$$F_v = 6376.5 \text{ N}$$

- iii) Cornering Force (lateral force due to cornering)

Assumption: Max 2g lateral acceleration

Cornering force = Vertical force = 6376.5 N

iv) Hard Braking

Assumption: use deceleration as calculated from new disc rotor = 0.66 m/s^2

$$F = (M_v/4) \times a \quad : M_v = 1300\text{kg} \quad a = 0.66 \text{ m/s}^2$$

$$F = 214.5 \text{ N}$$

v) Minor Collision (low speed collisions)

- a. Minor accident (rear bumper hit by another vehicle at less than 40 km/h)
- b. Minor frontal crash (hitting another car in front at less than 40 km/h)
- c. Minor side impact (minor fender bender collision at the side of the vehicle at less than 40 km/h)

vi) Torque on rotor (maximum torque delivered by motor)

Maximum Torque is 120 N.m and applied as a force on the slots holding the magnets.

$$F_{\text{average}} = T/R_{\text{average}}$$

vi) Maximum Rotor-Stator Attraction Force

Based on an estimate of the magnetic field strength (1.42 Tesla), the surface area of the magnets and the design air gap of 2 mm between the rotor and the stator, the maximum rotor stator attraction force is calculated to be 1962 N.

4.4 Preliminary Finite Element Analysis

4.4.1 Finite Element Analysis on Spindle

-Maximum vertical force of 6376.5 N, fully constrained at the 4 bolt holes and back plate.

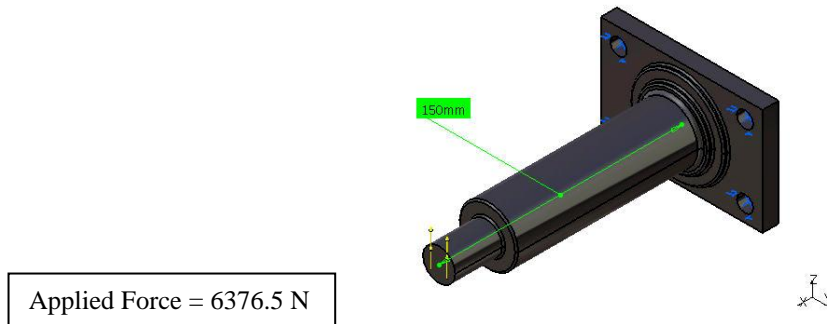


Figure 4.3: Maximum vertical loading on the spindle

Meshing & Results

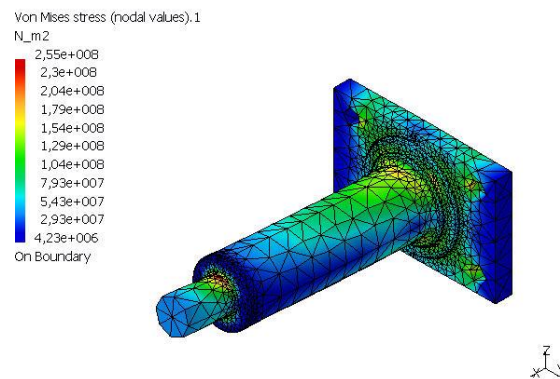


Figure 4.4: Von Mises Stress results on the spindle

Material use: High strength carbon steel (Yield Strength = 420 MPa)

Based on the above results, spindle didn't failed and design can be further optimized.

4.4.2 Finite Element Analysis on Casing Arm

Vertical force of 797.06 N at each arm, fully constrained at 4 bolt holes and back plate.

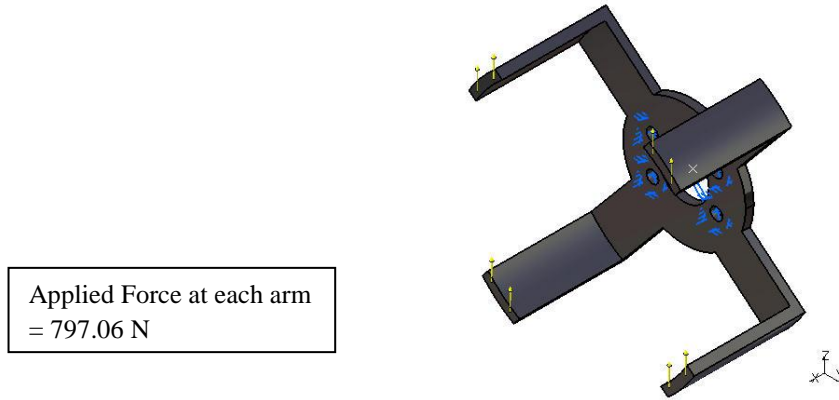


Figure 4.5: Maximum vertical load on casing arm

Meshing and Results

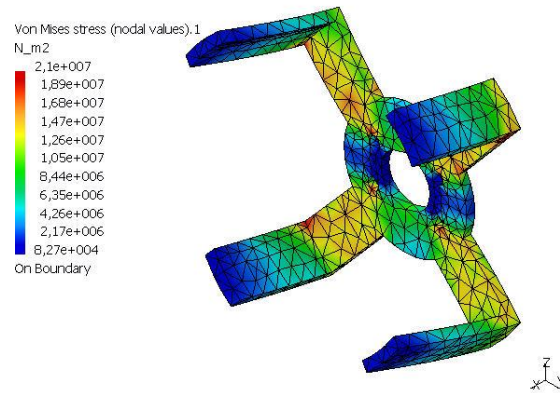


Figure 4.6: Von Mises stress results on casing arm

Material use: Mild steel (Yield Strength = 250 MPa)

Based on the results, the casing arm did not failed but there are areas where Von Mises stress is really high and need reinforcements.

4.5 Brake System Design Calculation

The braking design equations are used to first estimate the performance of the existing car. Later the same sets of equations are used to calculate the performance of the first design iteration for the new disc braking system and it is targeted that the performance of the new disc design braking system should approach the performance level shown by the existing brake system of the stock car. The calculations for section 4.5.1 are accomplished using actual perimeters and dimensions of the stock car brake system and it is found that the braking performance calculated is within reasonable values. However, actual testing need to be performed validates the design equations and assumptions used in the calculations.

4.5.1 Existing mechanical brake system on Proton Waja

Vehicle Mass = 1300kg

Starting Velocity = 100km/h

a. Kinetic Energy:

$$Kinetic\ Energy = \frac{1}{2} \times m_v \times v_v^2$$

U = 501,543 Joule

b. Brake Pedal Force (based on kinematic advantage of brake pedal):

$$F_{bp} = F_d \times \{L_2 \div L_1\}$$

; $F_d = 147.15\ N$ $L_2/L_1 = 2.272727$

$F_{bp} = 334\ N$

c. Pressure of master cylinder (based on actual dimension of the master cylinder):

$$P_{mc} = \frac{F_{bp}}{A_{mc}}$$

; Diameter master cylinder = 0.2 m

Area master cylinder = πr^2

$$P_{mc} = 10630 \text{ Pa}$$

- d. Pressure calliper (assumption that pressure losses is negligible in the brake line):

$$\text{Pressure calliper} = \text{Pressure of master cylinder} = 10630\text{Pa}$$

- e. Force at caliper:

$$F_{cal} = P_{cal} \times A_{cal}$$

; Diameter caliper = 0.25m

$$F_{cal} = 522 \text{ N}$$

- f. Force Clamping (clamping force at both sides):

$$F_{clamp} = F_{cal} \times 2$$

$$F_{clamp} = 1044 \text{ N}$$

- g. Force friction:

$$F_{friction} = F_{clamp} \times \mu_{bp}$$

; $\mu_{bp} = 0.55$

$$F_{friction} = 574.2 \text{ N}$$

- h. Rotor braking torque:

$$T_r = F_{friction} \times R_{eff}$$

; $R_{eff} = 0.11\text{m}$

$$T_r = 63.162 \text{ Nm}$$

- i. Torque at wheel and tire:

$$T_r = T_w = T_t = 63.162 \text{ Nm}$$

j. Force at tire:

$$F_{tire} = \frac{T_t}{R_t}$$

; $R_t = 0.3\text{m}$

$$F_{tire} = 210.54 \text{ N}$$

k. Total force:

$$F_{total} = \sum F_{tire\ LF, RF, LR, RR}$$

$$F_{total} = 842.16 \text{ N}$$

l. Deceleration of vehicle:

$$a_v = \frac{F_{total}}{m_v}$$

$$a_v = 0.65 \text{ m/s}^2$$

m. Stopping distance

$$SD_v = \frac{v_v^2}{2 \times a_v}$$

$$SD_v = 21.4\text{m}$$

Note: The braking distance is consistence which values published by some literatures.

4.5.2 New disc brake rotor analysis (without regenerative braking)

(Increase effective radius to 0.145 m and decrease caliper diameter to 0.22 m)

Vehicle Mass = 1300kg

Starting Velocity = 100km/h

- a. Kinetic Energy:

$$Kinetic\ Energy = \frac{1}{2} \times m_v \times v_v^2$$

$$U = 501,543\ \text{Joule}$$

- b. Brake Pedal Force:

$$F_{bp} = F_d \times \{L_2 \div L_1\}$$

$$; F_d = 147.15\ \text{N} \quad L_2/L_1 = 2.272727$$

$$F_{bp} = 334\ \text{N}$$

- c. Pressure of master cylinder:

$$P_{mc} = \frac{F_{bp}}{A_{mc}}$$

$$; \text{Diameter master cylinder} = 0.2\ \text{m}$$

$$\text{Area master cylinder} = \pi r^2$$

$$P_{mc} = 10630\ \text{Pa}$$

- d. Pressure calliper:

$$\text{Pressure calliper} = \text{Pressure of master cylinder} = 10630\ \text{Pa}$$

- e. Force at caliper:

$$F_{cal} = P_{cal} \times A_{cal}$$

$$; \text{Diameter caliper} = 0.22\ \text{m}$$

$$F_{cal} = 404\ \text{N}$$

f. Force Clamping:

$$F_{clamp} = F_{cal} \times 2$$

$$F_{clamp} = 808 \text{ N}$$

g. Force friction:

$$F_{friction} = F_{clamp} \times \mu_{bp}$$

$$; \mu_{bp} = 0.55$$

$$F_{friction} = 444.4 \text{ N}$$

h. Rotor braking torque:

$$T_r = F_{friction} \times R_{eff}$$

$$; R_{eff} = 0.145 \text{ m}$$

$$T_r = 64.438 \text{ Nm}$$

i. Torque at wheel and tire:

$$T_r = T_w = T_t = 64.438 \text{ Nm}$$

j. Force at tire:

$$F_{tire} = \frac{T_t}{R_t}$$

$$; R_t = 0.3 \text{ m}$$

$$F_{tire} = 214.79 \text{ N}$$

k. Total force:

$$F_{total} = \sum F_{tire \text{ LF, RF, LR, RR}}$$

$$F_{total} = 859.17 \text{ N}$$

- l. Deceleration of vehicle:

$$a_v = \frac{F_{total}}{m_v}$$

$$a_v = 0.66 \text{ m/s}^2$$

- m. Stopping distance

$$SD_v = \frac{v_v^2}{2 \times a_v}$$

$$SD_v = 21 \text{ m}$$

4.5.3 New disc brake rotor in combination with regenerative braking from the motor

(Increase effective radius to 0.145 m and decrease caliper diameter to 0.22 m)

(Additional regenerative braking torque of 50 N.m (total 100 N.m for both) per in-wheel motor at 100 amps charging current into the batteries)

Vehicle Mass = 1300kg

Starting Velocity = 100km/h

- n. Kinetic Energy:

$$Kinetic \ Energy = \frac{1}{2} \times m_v \times v_v^2$$

$$U = 501,543 \text{ Joule}$$

- o. Brake Pedal Force:

$$F_{bp} = F_d \times \{L_2 \div L_1\}$$

$$; F_d = 147.15 \text{ N} \quad L_2/L_1 = 2.272727$$

$$F_{bp} = 334 \text{ N}$$

p. Pressure of master cylinder:

$$P_{mc} = \frac{F_{bp}}{A_{mc}}$$

; Diameter master cylinder = 0.2 m

$$\text{Area master cylinder} = \pi r^2$$

$$P_{mc} = 10630 \text{ Pa}$$

q. Pressure calliper:

$$\text{Pressure calliper} = \text{Pressure of master cylinder} = 10630 \text{ Pa}$$

r. Force at caliper:

$$F_{cal} = P_{cal} \times A_{cal}$$

; Diameter caliper = 0.22m

$$F_{cal} = 404 \text{ N}$$

s. Force Clamping:

$$F_{clamp} = F_{cal} \times 2$$

$$F_{clamp} = 808 \text{ N}$$

t. Force friction:

$$F_{friction} = F_{clamp} \times \mu_{bp}$$

; $\mu_{bp} = 0.55$

$$F_{friction} = 444.4 \text{ N}$$

u. Rotor braking torque:

$$T_r = F_{friction} \times R_{eff} \quad ; R_{eff} = 0.145\text{m}$$

$$T_r = 64.438 \text{ Nm (only from mechanical braking)}$$

v. Torque at wheel and tire:

$$T_r = T_w = T_t = 64.438 \text{ Nm (only from mechanical braking)}$$

w. Force at tire:

$$F_{tire} = \frac{T_t}{R_t} \quad ; R_t = 0.3\text{m}$$

$$F_{tire} = 214.79 \text{ N (only from mechanical braking)}$$

x. Total force:

$$F_{total} = \sum F_{tire\ LF, RF, LR, RR}$$

$$F_{total_mech} = 859.17 \text{ N (only from mechanical braking)}$$

$$F_{total_regen} = 100 \text{ N.m} / 0.3 \text{ m} = 333.33 \text{ N}$$

$$F_{total} = 859.17 + 333.33 \text{ N} = 1192.5 \text{ N}$$

y. Deceleration of vehicle:

$$a_v = \frac{F_{total}}{m_v}$$

$$a_v = 0.92 \text{ m/s}^2$$

z. Stopping distance

$$SD_v = \frac{v_v^2}{2 \times a_v}$$

$$SD_v = 15.1 \text{ m}$$

Based on the above calculations, the new disc rotor braking system in combination with regenerative braking will have a stopping distance of 15.1 m (which is 6.3 m less than the stock vehicle). This shows that the brake components of the new disc braking system can be further reduced in size.

4.6 Component Sizing for Critical Parts

4.6.1 Bending Moment (Spindle)

$$d = 15 \text{ mm}, m = 1300 \text{ kg}, g = 9.81 \text{ m/s}^2, \sigma_{\max} = 210 \text{ MPa}$$

$$F_{\text{vertical}} = (m/4) \times 2g = 6376.5 \text{ N}$$

$$\sigma_{\max} = (32 \times F_v \times d) / \pi D^3 = 210 \text{ MPa}$$

$$D = 0.0359 \text{ m}$$

4.6.2 Arm (Rectangle)

$$A = 0.05 \times 0.01 = 5 \times 10^{-4} \text{ m}^2, r_i = 0.05 \text{ m}, r_o = 0.06 \text{ m}, \acute{r} = 0.055 \text{ m}, C_i = 4.85 \times 10^{-3} \text{ m}, \\ e = 1.52 \times 10^{-4} \text{ m}$$

$$\int \text{area } dA/p = A_1 = t \times \ln(r_i / r_o) = 9.12 \times 10^{-3} \text{ m}^2$$

$$r_n = A / A_1 = 0.05485 \text{ m}$$

$$\sigma = Mc_i / (e \times A \times r_i) = 159.69 \text{ MPa}$$

$$\sigma \times 2 = 305.37 \text{ MPa} \leq 420 \text{ MPa} \quad \text{*Component sizing accepted}$$

4.6.3 Torsion

$$T = 120 \text{ Nm}, r = 0.058 \text{ m}, D_o = 0.138 \text{ m}, D_i = 0.09 \text{ m}, J = 2.92 \times 10^{-5}$$

$$\tau = (T \times r) / J = 236.9 \text{ kPa} \quad S_f \times \tau \leq S_y$$

4.6.4 Shear Force

$$T = 120 \text{ Nm}, r = 0.058 \text{ m}, A_{\text{bolt}} = 5 \times 10^{-5} \text{ m}^2$$

$$F_{\text{bolt}} = T/r = 2084.021 \text{ N}$$

$$\tau = (F_{\text{bolt}}/n) / A_{\text{bolt}} \leq 210 \text{ MPa}$$

$$n = 0.2 \approx 1 \text{ bolt or more}$$

CATIA 3D drawings for new design (Design B):

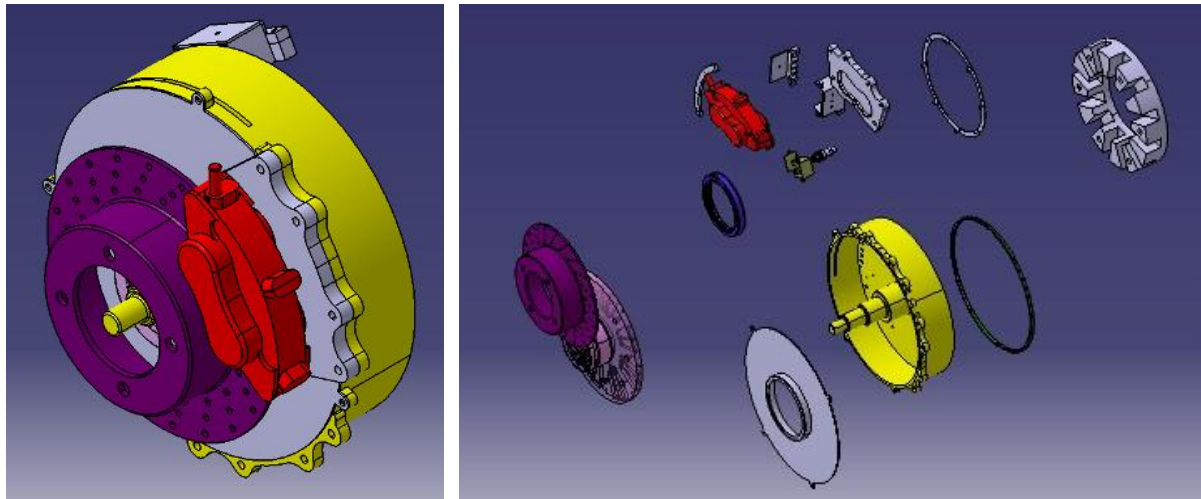


Figure 4.7: Isometric View and Exploded View of the new In-Wheel Motor Assembly

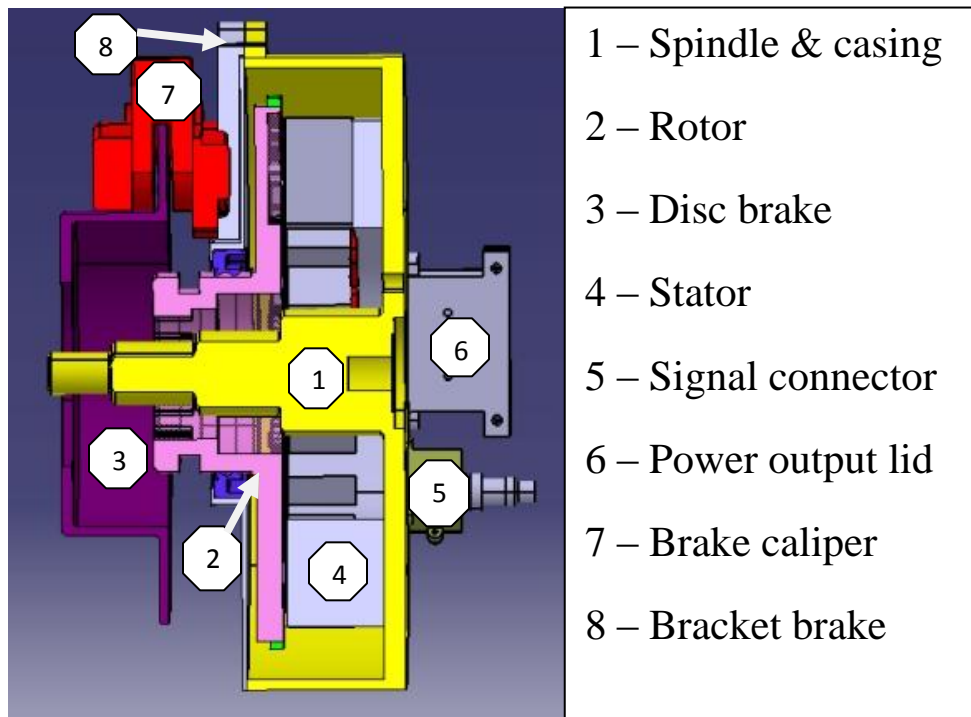


Figure 4.8: Section view of the new In-Wheel motor assembly

4.7 Materials used

Table 4.2: Material properties of the rotor, casing and bracket

AISI 410		
Mechanical Property Requirements For Material in the Annealed and Heat Treated		
Tensile Strength Mpa Min Max		0.2% Yield Strength Mpa Min
700 850		495
Typical Mechanical Properties At Room Temperature - *Hardened and Tempered		
Tensile Strength Mpa		0.2% Yield Strength Mpa
760		595

- From the above table shown typically the yield strength is over 500 MPa depending on treatment. Meanwhile the typical yield strength for mild steel is 250 MPa and aluminum alloy 6061 T6 is 240 MPa which are smaller than heat treated AISI 410. For the critical components, the higher yield strength material is critical to reduce the mass and AISI 410 is selected for this reason.

4.8 Design Optimization

4.8.1 Critical Part Design

Rotor (Torsion stress)

- Maximum rotational force of 526.316 N, fully constrained at the hole

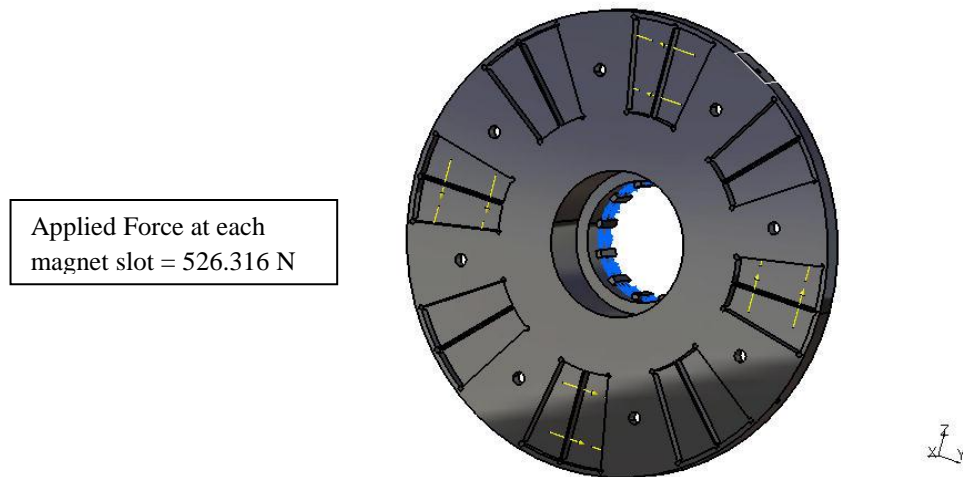


Figure 4.9: Maximum rotational loading on the rotor

Finite element analysis

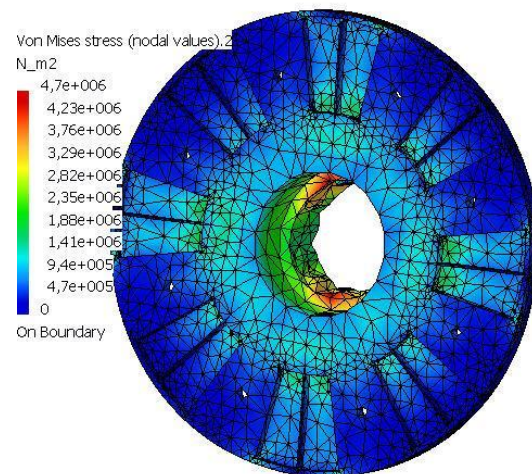


Figure 4.10: Von Mises stress results on rotor

- Based on the maximum Von Mises stress results of $4.7 \times 10^6 \text{ N/m}^2$, the component is sufficiently designed to withstand the maximum forces of 526.316 N under ‘stalling’ condition (given typical stainless steels AISI 410 material strength of $5 \times 10^8 \text{ N/m}^2$) and clearly this component design can be further optimized to reduce the total mass. The maximum displacement under this loading condition is 0.00406 mm and is acceptable under this type of rotational loading condition.

Rotor (magnet)

- Maximum rotational force of 1962 N, fully constrained at the hole

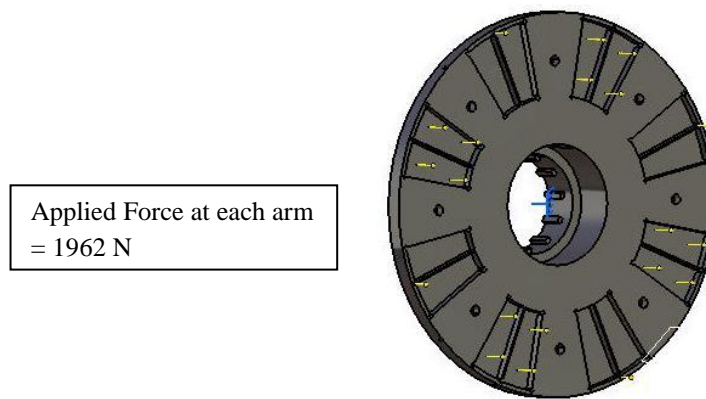


Figure 4.11: maximum loading on the rotor

Finite element analysis

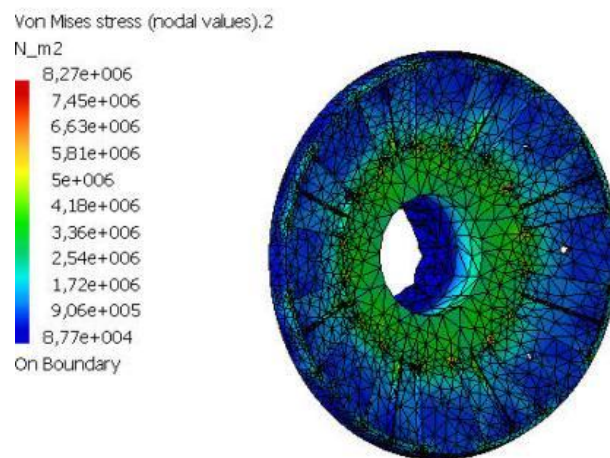


Figure 4.12: Von Mises stress result on motor

- Based on the maximum Von Mises stress results of $8.27 \times 10^6 \text{ N/m}^2$, the component is sufficiently designed to withstand the exerted force of 1962 N (given typical stainless steels AISI 410 material strength of $5 \times 10^8 \text{ N/m}^2$) and clearly this component design can be further optimized to reduce the total mass. The maximum displacement under this loading condition is 0.0105 mm and is acceptable under the tight tolerance requirement of the air gap distance.

Cross section of internal stress

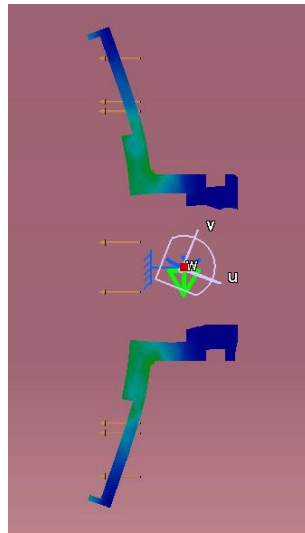


Figure 4.13: cross section on rotor

Rotor (frequency analysis)

Modal Analysis Results

Table 4.3: Natural Frequencies based on modal analysis

No.	Mode	Frequency (Hz)
1	1	1821.28
2	2	1874.09
3	3	1877.47
4	4	2134.55
5	5	2279.90
6	6	3062.62
7	7	3071.88
8	8	4276.02
9	9	4823.71
10	10	4914.91

- The resonance which is expected when the rotor hit the natural frequencies will caused undesired deformation of the rotor. This is very critical because the air gap length between the rotor and stator is very small at only 2 mm. Based on the results, the first natural frequency is at 1821 Hz and this is much higher than the maximum operating frequencies of the rotor ($1 \text{ Hz} = \text{rpm}/60$ meaning that maximum speed of 1800 rpm corresponds to only 30 Hz).

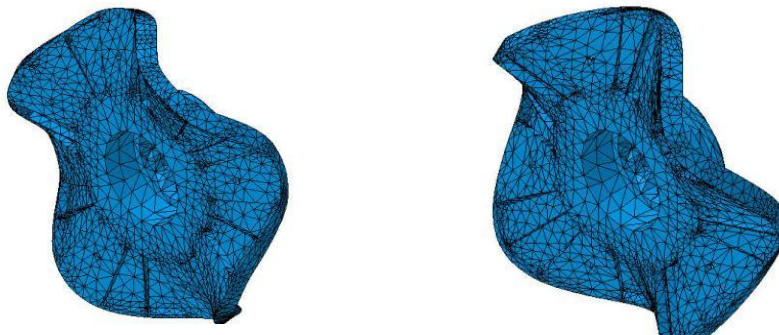


Figure 4.14: Examples of rotor deformation from modal analysis

Design modification for rotor

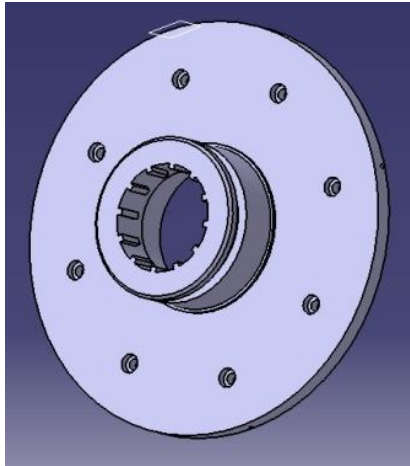


Figure 4.15: Actual Rotor

Objectives

- Maximum stress on the component not to exceed the yield strength of the materials by the minimum safety factor of 2.0 and the maximum displacement not to exceed 0.2 mm.
- To reduce the total mass

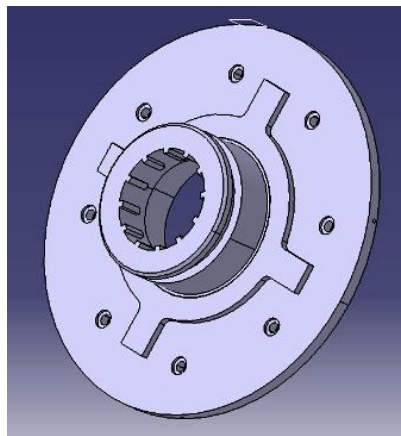


Figure 4.16: 1-rotor modified design

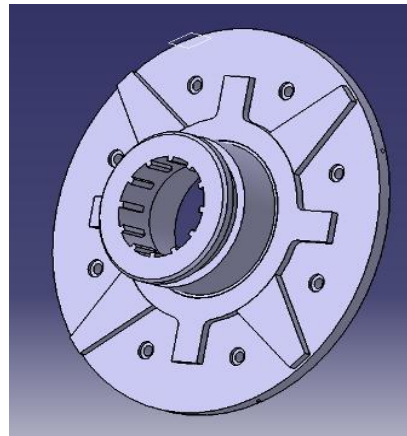


Figure 4.17: 2-rotor modified design

Modifications

- Figure above shown the new designs modification for rotor
- 1-rotor modified design
 - Thickness of rotor is reduced by 3 mm
 - Feature added (as shown on figure 4.16)
- 2-rotor modified design
 - Modification from 1-rotor modified design.
 - Added four new features longer up until the end of radius (as shown in figure 4.17)
 - Little bit heavier than 1-rotor modified design
- Reduce the thickness mean reduce the total mass of the rotor

Analysis

Stress (rotational)

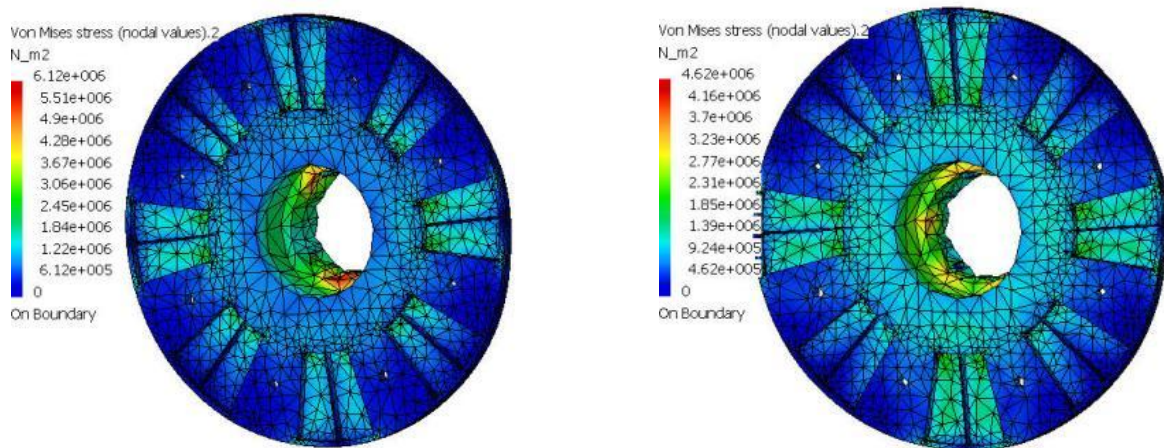


Figure 4.18: Von Mises stress result on 1, 2-rotor modified design

- Based on the maximum Von Mises stress results of 1-rotor modified design is $6.12 \times 10^6 \text{ N/m}^2$, higher than actual rotor which is $4.7 \times 10^6 \text{ N/m}^2$, but different for 2-rotor modified design the Von Mises stress result is $4.62 \times 10^6 \text{ N/m}^2$, which is smaller than actual rotor. Rationally the component design of 2-rotor modified give the better result compared to actual and 1-rotor modified design.

Stress (Magnet)

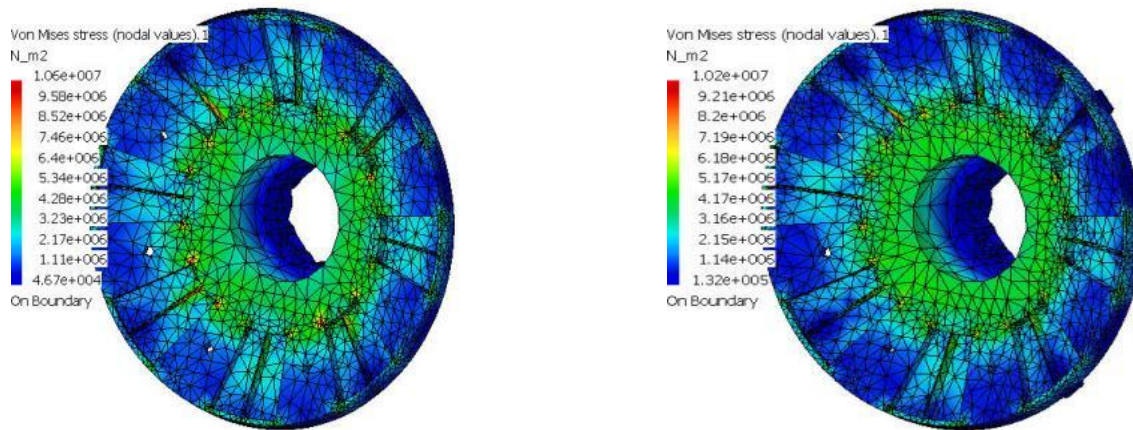


Figure 4.19: Von Mises stress result on 1, 2-rotor modified design

- Based on the maximum Von Mises stress results of 1-rotor modified design is $1.06 \times 10^7 \text{ N/m}^2$, and 2-rotor modified design is $1.02 \times 10^7 \text{ N/m}^2$ both are higher than actual rotor which is $8.27 \times 10^6 \text{ N/m}^2$. The maximum displacement under this loading condition for modified rotors, 0.0149 mm and 0.0141 mm which are slightly higher than actual rotor loading condition of 0.0105 mm. Both modified designs should still sufficiently design to withstand the exerted force of 1962 N and smaller total mass than actual rotor.

Cross Section view of internal stress

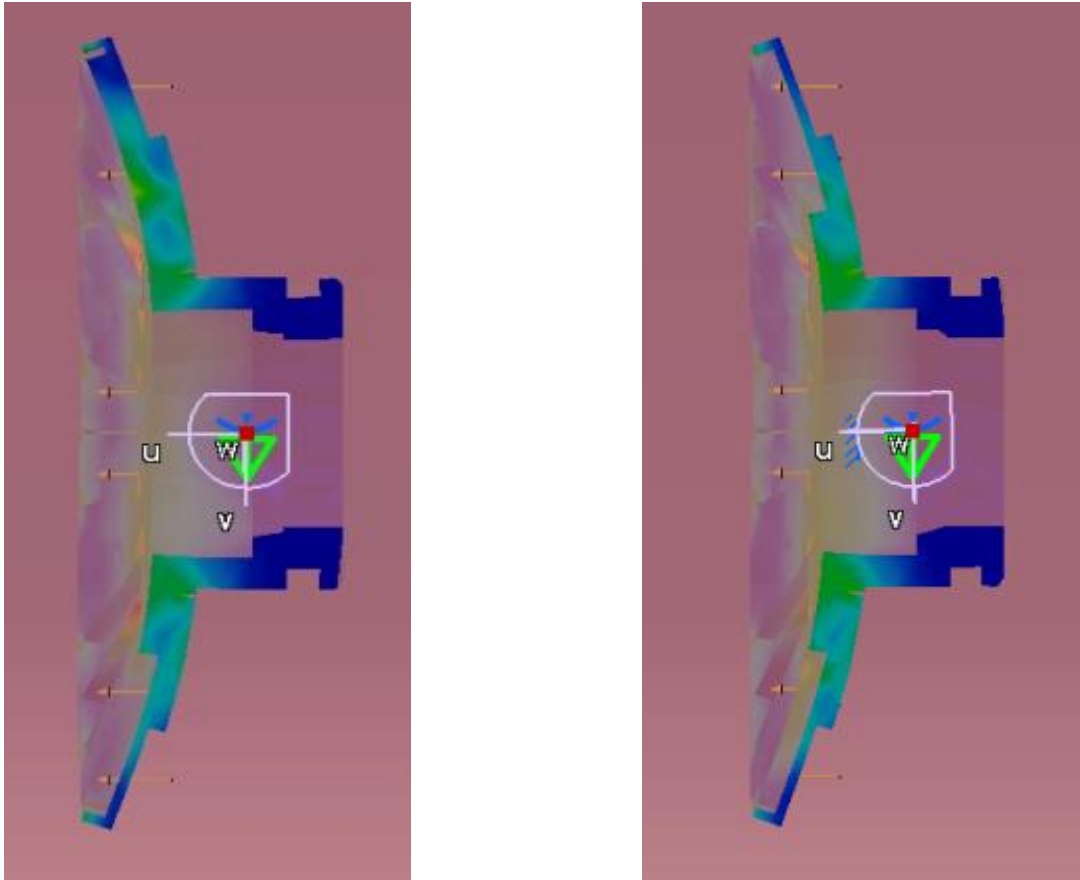


Figure 4.20: Section view for stress result on 1, 2-rotor modified design

After consider several analyses, the 2nd modified design of rotor gives the best result of design optimization.

Casing and Spindle

- Maximum vertical force of 9810 N, fully constrained at the 4 holes

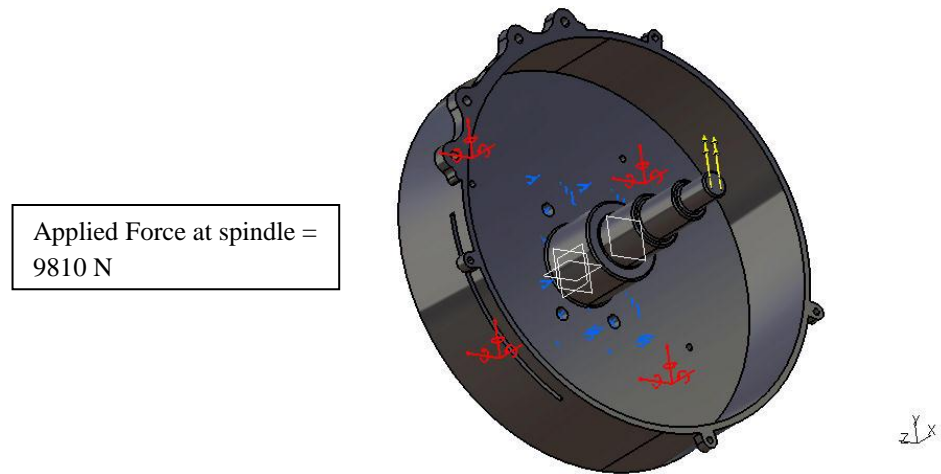


Figure 4.21: Maximum rotational loading on the spindle

Finite element analysis

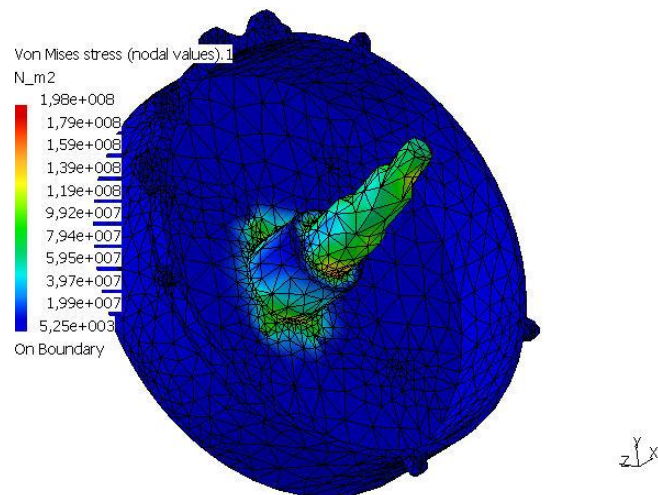


Figure 4.22: Von Mises stress results on spindle

Cross section view of internal stress

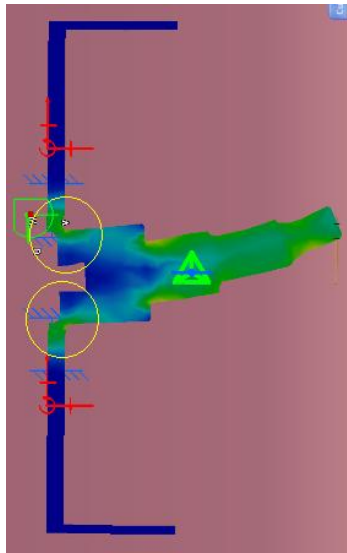


Figure 4.23: Cross section on casing and spindle

- Based on the maximum Von Mises stress results of $1.98 \times 10^8 \text{ N/m}^2$, the component is sufficiently designed to withstand the maximum forces of 9810 N condition (given typical stainless steels AISI 410 material strength of $5 \times 10^8 \text{ N/m}^2$) and clearly this component design can be further optimized to protect the critical part (yellow circles).

Design modification for casing and spindle

Objectives

- Maximum stress on the component not to exceed the yield strength of the materials by the minimum safety factor of 2.0 and the maximum displacement not to exceed 1 mm.

Modification

- Added new diameter of 60mm and extruded for 6.5mm at spindle
- Maximum vertical force of 9810 N, fully constrained at the 4 holes

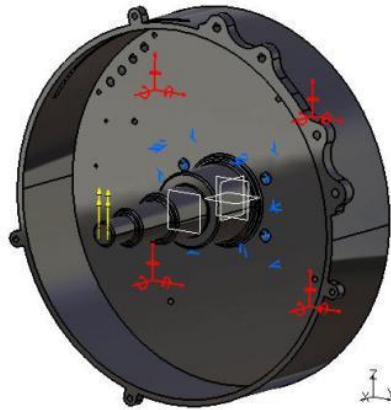


Figure 4.24: Modified design of casing and spindle

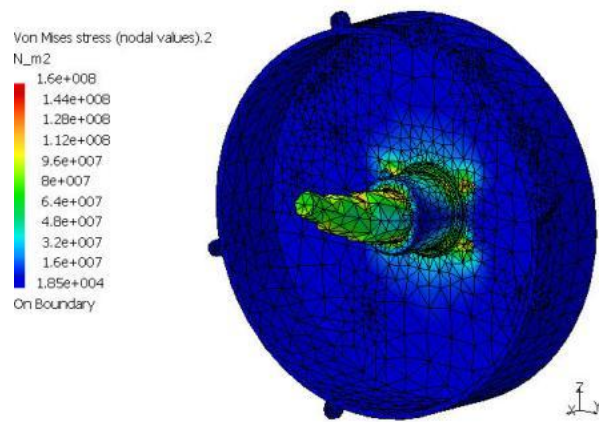


Figure 4.25: Von Mises stress result on casing and spindle

Cross section view of internal stress

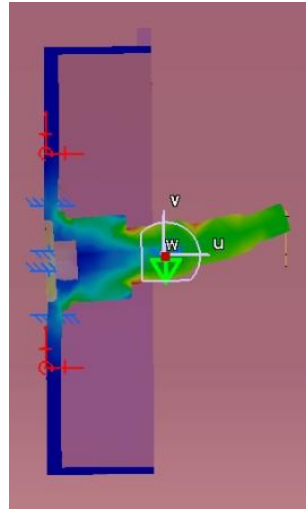


Figure 4.26: Section view of casing and spindle

- Based on the maximum Von Mises stress results of $1.6 \times 10^8 \text{ N/m}^2$ of modified design, the component is sufficiently designed to withstand the maximum forces of 9810 N (given typical stainless steels AISI 410 material strength of $5 \times 10^8 \text{ N/m}^2$) and clearly this modified component design is safely protected under this type of loading condition.

Thermal analysis (ANSYS)

Temperature of 200 °C is applied at the inner back plate of the casing as this is expected to be the maximum operating temperature of the stator. The main objective of this analysis is to predict the temperature distribution on the casing. There are limitations of this analysis since it is performed only on a single component without considering the interaction between the casing, stator, coils, bearings, suspension arm and the rotor. Regardless, the results obtained should be sufficient to be used in the decision on heat sink design at the outer sections of the casing.

Temperature distribution results

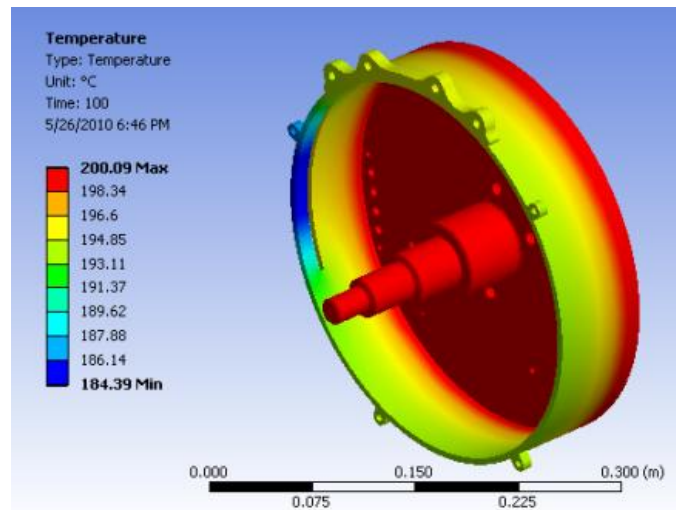


Figure 4.27: Front view for thermal analysis using ANSYS

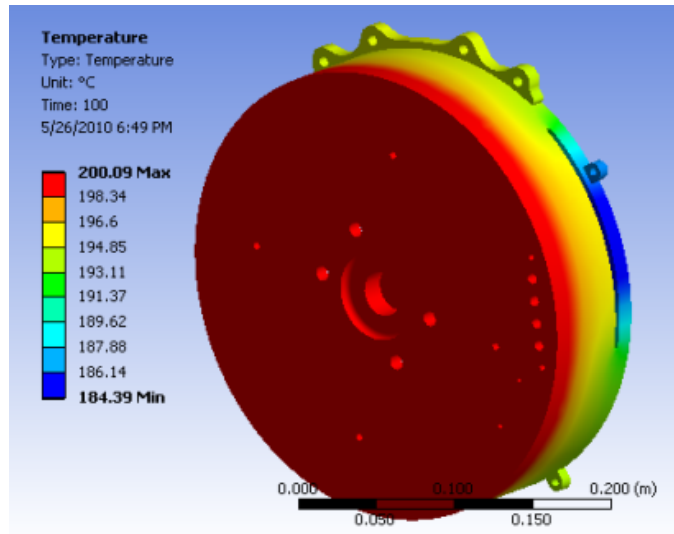


Figure 4.28: Back view for thermal analysis using ANSYS

Based on the temperature distribution obtained, the maximum temperatures are at the back of the casing as expected. The temperature of the spindle is also very high and this is not desired since it will affect the bearing and the rotor which holds the magnets (maximum operating temperature of the magnets is only 100 °C). Based on the results shown in the figures above, the heat sink design must be able to dissipate the heat quickly and more efficiently through the back and around the casing to reduce heat transfer towards the spindle.

Heat flux results

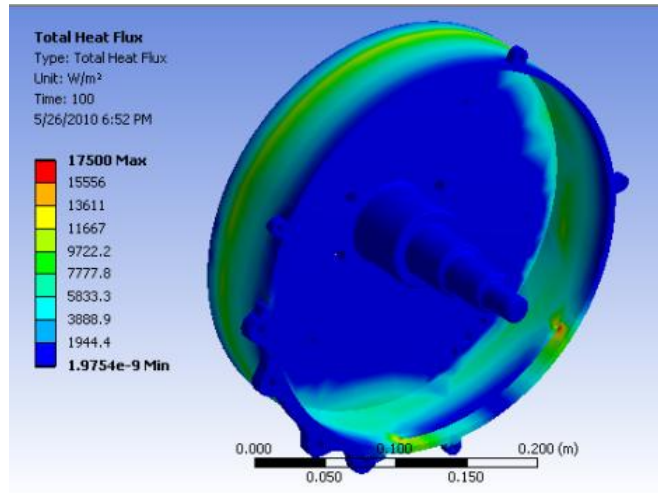


Figure 4.29: Front view for heat flux using ANSYS

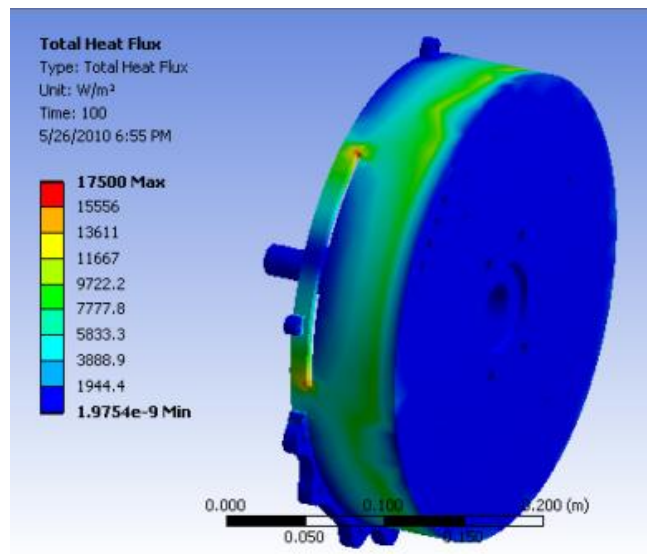


Figure 4.30: Back view for heat flux using ANSYS

Design modification for casing and spindle on thermal analysis

Modification

- Added a new feature (fins) on back of casing

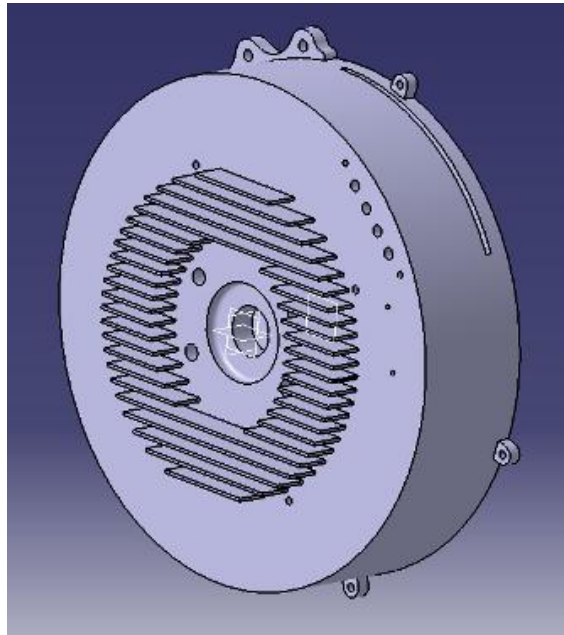


Figure 4.31: Fins attached on casing

- Based on the above figure shown the modification by added a new heat sink (fins) at the back of the casing. It is because to dissipate the heat quickly and to reduce heat transfer towards the spindle. It can be more efficiently if the heat sink also added around the casing.

Bracket

- Maximum rotational force of 2272.278 N, fully constrained at the 4 holes

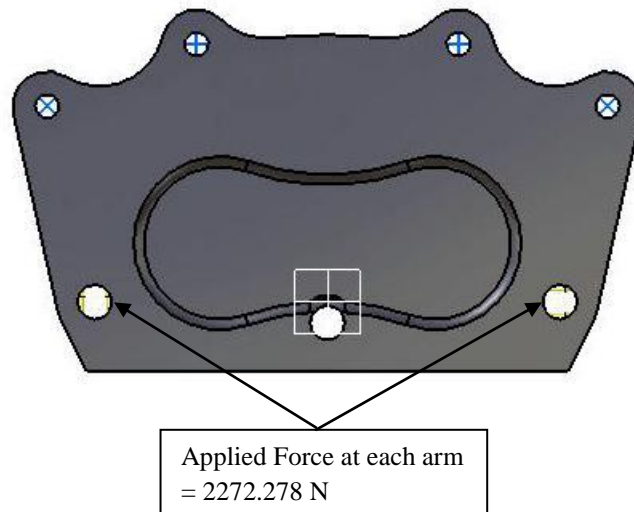


Figure 4.32: Maximum rotational loading on the bracket

Finite element analysis

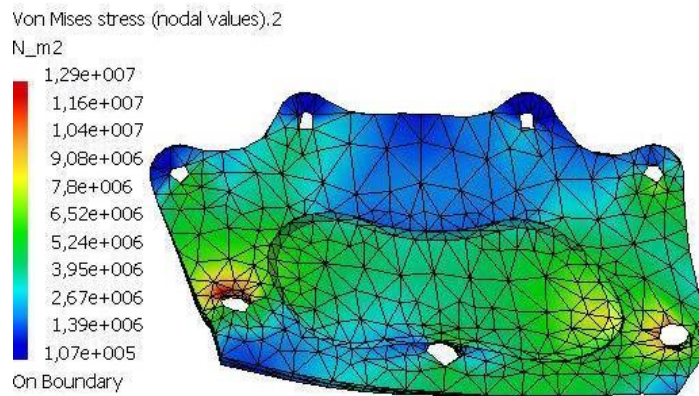


Figure 4.33: Von Mises stress results on bracket

- Based on the results, the bracket did not failed but there are areas where Von Mises stress is really high and design reinforcements are required.

4.9 Discussion

Generally, the new selected concept compared to previous design concept for the in-wheel motor also seems to be able to address most of the technical challenges and limitations. The final results shown above indicate that the motor components can withstand the expected types of loadings likely encountered during operation of the vehicle. In detail, improvements and optimizations are already been done toward new concept. Finally the design has been analyzed further in detail to minimize the magnitude of the stress and to reduce the components mass.

The brake system calculation shows that the new larger new disc brake most likely will outperformed the original brake system when used in combination with the regenerative braking from the motor. The new disc rotor braking system in combination with regenerative braking will have a stopping distance of 15.1 m compared to the stopping distance new disc brake rotor analysis only which is 21 m.

CHAPTER 5

CONCLUSION AND RECOMMENDATION

5.1 Conclusion

Based on the literature studies, research resources and completed overall analyses, the objectives of the project are successfully achieved within a period of two semesters. After completed all analyses, the selected configuration for the in-wheel motor will be able to be packaged nicely within the target vehicle available design volume (inside the rear wheel arch of a Proton Waja). The sizing of the components was earlier determined using analytical stress calculations and later it was verified that most likely the components will not fail under the typical loadings in normal operating conditions of the vehicle. In addition, the design optimization of these components has been conducted in order to reduce the stress magnitudes and the overall mass of the in-wheel motor. Thermal analysis result indicates that good heat sink design is necessary to dissipate heat generated from the motor.

5.2 Recommendation

Previously this project was intended to include fabrication of the motor prototype, but due to the time constraint the main task were reduced to cover only the design and analysis processes. Nevertheless, the prototype fabrication stage is important in order to verify the design and to test the prototype. It is highly recommended that fabrication of a mock-up prototype followed by the fabrication of a revised working prototype would be the next logical step of the development of this motor.

REFERENCES

- [1] Schafer, A. (1998), *"The global demand for motorized mobility."*, Transportation Research A 32(6), page 455-477.
- [2] National Research Council (U.S.). Standing Committee to Review the Research Program of PNGV (1998), *"Review of the research program of the Partnership for a New Generation of Vehicles: Fourth Report"*, National Academies Press, page 77.
- [3] L. Ulrich, *"They're Electric, but Can They Be Fantastic?"*, The New York Times, published on 23rd September, 2007 (Available at <http://select.nytimes.com/preview/2007/09/23/automobiles/1154690129008.html>)
- [4] Press Release (1999), *"NGM Drive System's Superior Performance Demonstrated in Solar Car Races"*, (New Generation Motors Corporation <http://www.ngmcorp.com>).
- [5] R. A. Cooper (1998), *"Wheelchair selection and configuration"*, Demos Medical Publishing, page 234.
- [6] J. L. Flatley (2009), *"E-Traction's in-wheel motor sportin' hybrid electric bus"*, (Available at <http://www.engadget.com/2009/03/23/e-tractions-in-wheel-motor-sportin-hybrid-electric-bus/>)
- [7] Recycling Technologies (2003), *"Latest MMC technologies and near-future goals"*, (available at http://www.mitsubishi-motors.com/corporate/about_us/technology/environment/e/miev.html)
- [8] D. Yoney (2009), *"What are in-wheel motors?"*, (Available at <http://green.autoblog.com/2009/08/06/greenlings-what-are-in-wheel-motors/>)
- [9] Stoptech (1999), *"Formulas for Vehicle Braking Dynamics"*, (available at http://www.stoptech.com/tech_info/formulas%20vehicle_braking_dynamics.pdf)
- [10] Wikipedia (2010), *"Regenerative brake"*, (available at http://en.wikipedia.org/wiki/Regenerative_brake)

- [11] Insight central (2008), “*Deceleration / Regenerative Braking Mode*”, (available at <http://www.insightcentral.net/encyclopedia/enregenerativebraking.html>)
- [12] Adrian Chernoff (2002), “*General Motors AUTONOMY: Sports Coupe*”, (available at <http://www.adrianchernoff.com/pages/AUTOnomy.html>)
- [13] Sandeep Dhameja (2002), “*Electric vehicle battery systems*”, Newnes (page 24).
- [14] J. F. Gieras (2008), “*Axial Flux Permanent Magnet Brushless Machines – 2nd Edition*”, Springer.

APPENDICES

Appendix 1

Gantt Charts

GANTT CHART

FIRST SEMESTER OF 2 SEMESTER FINAL YEAR PROJECT

Detail of week	1	2	3	4	5	6	7	8	9	10	11	12	13	14	SW	EX
Introduction on the FYP title Receive proposal and document from supervisor	■	■														
ANSYS training Preliminary research work			■	■	■	■										
Submission of preliminary report				■												
Data gathering In wheel motor Brake system – mechanical & regenerative Axial flux permanent magnet				■	■	■										
Target design specification Submission of progress report						■	■	■	■	■						
Design Selection										■	■					
Design process Analytical calculation Stress analysis											■	■	■			
Submission of interim report													■			
Oral presentation														■	■	

GANTT CHART

SECOND SEMESTER OF 2 SEMESTER FINAL YEAR PROJECT

Detail of week	1	2	3	4	5	6	7	8	9	10	11	12	13	14	SW	EX
Design optimization		■	■	■	■	■	■									
Submission of progress report 1					■											
Design iteration						■	■	■	■	■						
Submission of progress report 2									■							
Design modification										■	■					
Finalized design											■	■	■			
Submission of dissertation final draft													■			
Oral presentation														■	■	
Submission of project dissertation (hardbound)																■